OPEN ACCESS

Original research

Human milk oligosaccharide 2′-fucosyllactose protects against high-fat diet-induced obesity by changing intestinal mucus production, composition and degradation linked to changes in gut microbiota and faecal proteome profiles in mice

Paola Paone ,[1] Dimitris Latousakis ,[2] Romano Terrasi,[3] Didier Vertommen ,[4] Ching Jian ,[5] Valentina Borlandelli ,[6] Francesco Suriano ,[7] Malin E V Johansson ,[7] Anthony Puel,[1,8] Caroline Bouzin ,[9] Nathalie M Delzenne ,[1] Anne Salonen ,[5] Nathalie Juge ,[2] Bogdan I Florea ,[6] Giulio G Muccioli ,[3] Herman Overkleeft ,[6] Matthias Van Hul ,[1,8] Patrice D Cani [1,8,10]

► Additional supplemental material is published online only. To view, please visit the journal online (https://doi.org/10.1136/gutjnl-2023-330301).

For numbered affiliations see end of article.

Correspondence to
Professor Patrice D Cani, Louvain Drug Research Institute (LDRI), Metabolism and Nutrition research group (MNUT), UCLouvain, Université catholique de Louvain, Avenue E. Mounier, 73 B1.73.11 B-1200, Brussels, Belgium; patrice.cani@uclouvain.be

AS, NJ, BIF, GGM, HO and MVH are joint senior authors.

Received 17 May 2023
Accepted 27 April 2024

To cite: Paone P, Latousakis D, Terrasi R, *et al*. *Gut* Epub ahead of print: [*please include* Day Month Year]. doi:10.1136/gutjnl-2023-330301

ABSTRACT

Objective To decipher the mechanisms by which the major human milk oligosaccharide (HMO), 2′-fucosyllactose (2′FL), can affect body weight and fat mass gain on high-fat diet (HFD) feeding in mice. We wanted to elucidate whether 2′FL metabolic effects are linked with changes in intestinal mucus production and secretion, mucin glycosylation and degradation, as well as with the modulation of the gut microbiota, faecal proteome and endocannabinoid (eCB) system.

Results 2′FL supplementation reduced HFD-induced obesity and glucose intolerance. These effects were accompanied by several changes in the intestinal mucus layer, including mucus production and composition, and gene expression of secreted and transmembrane mucins, glycosyltransferases and genes involved in mucus secretion. In addition, 2′FL increased bacterial glycosyl hydrolases involved in mucin glycan degradation. These changes were linked to a significant increase and predominance of bacterial genera *Akkermansia* and *Bacteroides*, different faecal proteome profile (with an upregulation of proteins involved in carbon, amino acids and fat metabolism and a downregulation of proteins involved in protein digestion and absorption) and, finally, to changes in the eCB system. We also investigated faecal proteomes from lean and obese humans and found similar changes observed comparing lean and obese mice.

Conclusion Our results show that the HMO 2′FL influences host metabolism by modulating the mucus layer, gut microbiota and eCB system and propose the mucus layer as a new potential target for the prevention of obesity and related disorders.

WHAT IS ALREADY KNOWN ON THIS TOPIC

⇒ High-fat diet-induced obesity and metabolic disorders is associated with alterations in microbiota profile and gut barrier function.
⇒ The intestinal mucus layer is altered during high-fat diet (HFD), western-style diet, low-fibre diet, emulsifier treatments and in genetically obese (*ob/ob*) mice and human with dysglycaemia. The alterations observed include increased penetrability, decreased thickness, reduced growth and different mucin glycans composition.
⇒ Prebiotic treatments such as 2′-fucosyllactose (2′FL) improved gut barrier integrity in an in vitro model by affecting the mucus layer, but no studies have investigated whether the mucus is involved in the protection against obesity in vivo.

INTRODUCTION

Obesity is associated with several metabolic alterations like type 2 diabetes, cardiovascular diseases and changes in the gut microbiota composition and gut barrier disruption.[1] Among the components of the gut barrier, it has been shown that the mucus layer is altered when the mice are fed a high-fat diet (HFD), western-style diet (WSD) or low-fibre diet and in *ob/ob* mice, as well as in patients with dysglycaemia. Among the alterations, it has been observed a reduced thickness, increased penetrability and altered mucin glycan composition.[2–9] The mucus exerts important roles in gut barrier protection and represents the interface of communication between bacteria and host. It is produced by the goblet cells (GCs) and constituted of glycoproteins called mucins, among which the main component is the secreted Muc2. The transmembrane mucins, involved in glycocalyx formation, are other important components of the gut barrier, conferring cell protection and mediating host–microbe interactions.[10] Mucins are glycosylated thanks to

WHAT THIS STUDY ADDS

⇒ This study shows that supplementing 2′FL to HFD reduces the increase in body weight and fat mass, attenuates glucose intolerance and affects hormones involved in appetite regulation and energy homeostasis.
⇒ 2′FL supplementation affects the mucus layer in vivo in the context of obesity, by increasing mucus production, secreted and transmembrane mucins, glycosyltransferases and glycosyl hydrolases, and mucin glycosylation.
⇒ Bacterial communities in mice fed with HFD plus 2′FL are remarkably enriched in *Akkermansia* and *Bacteroides* genera.
⇒ 2′FL supplementation changes faecal proteome profiles, increasing proteins involved in carbon, amino acids and fat metabolism and decreasing those involved in protein digestion and absorption.
⇒ Supplementing 2′FL affects the intestinal endocannabinoid system.

HOW THIS STUDY MIGHT AFFECT RESEARCH, PRACTICE OR POLICY

⇒ 2′FL is a prebiotic found naturally in the breast milk of about 80% of mothers. Excluding water, human milk oligosaccharides are the third most abundant ingredient in breast milk after fat and carbohydrates. Understanding their mechanism of actions and effects is vital information.
⇒ There is increased interest in 2′FL to be used as a supplement, not only in infant formula but also for subjects with 2′FL synthesis deficiency (ie, *Fut2* genetic polymorphisms inducing fucosyltransferase inactivity).
⇒ This study shows that the mechanisms by which 2′FL counteracts obesity and metabolic disorders are associated with changes in the intestinal mucus layer and points towards the mucus as a new potential therapeutic target for the prevention and/or treatment of obesity and metabolic disorders.

glycosyltransferases and mucin glycans supply attachment sites and allow bacterial growth and colonisation. Indeed, bacteria are able to produce glycosyl hydrolases (GHs) to degrade mucin glycans and use them as energy source.[10]

α−1,2-fucosyltransferase, encoded by the *FUT2* gene, is one of the glycosyltransferases responsible for the presence of histo-blood group antigens on multiple organs and on the gastrointestinal mucosa.[11] In recent years, genome-wide association studies have underlined the importance of FUT2 biology and showed that different polymorphisms may result in distinct secretor status, associated with the development of pathophysiology such as intestinal inflammation.[12] Furthermore, FUT2 has been shown to have significant effects on the intestinal bacterial community composition.[12–15] One of the major prototypical secretor-type oligosaccharides is the human milk oligosaccharide (HMO) 2′-fucosyllactose (2′FL).[16 17] In vivo and in vitro studies showed that 2′FL exerts biological properties as prebiotic, antibacterial, antiviral and immunomodulating effects and modifies the host's epithelial cell-surface glycome.[18] This has prompted an increased interest in 2′FL as HMO source in infant formula and, more recently, 2′FL is also being investigated in pathological contexts.[19] For example, in mice fed HFD, it was observed that 2′FL reduced body weight and fat mass gain.[20 21] In addition, 2′FL protected against gut barrier disruptions induced by inflammatory stimuli, by increasing GCs number and *Muc2* expression.[22 23] Further in vivo studies exploring the role of 2′FL on the mucus layer in the context of obesity induced by HFD feeding are still lacking.

To fill this gap, we designed a study aimed at deciphering whether the impact of 2′FL on metabolism could be linked to changes in the intestinal mucus production, glycosylation, secretion and degradation. In addition, we explored whether the effects on mucus layer and metabolism might be associated with modifications in gut microbiota composition, faecal proteome and endocannabinoid (eCB) system.

We believe that a comprehensive investigation into the intricate mechanisms of the mucus layer, including its biosynthesis, turnover and degradation, may offer novel insights into developing efficacious interventions for mitigating or preventing obesity and related metabolic disorders.

RESULTS

2′FL counteracts metabolic alterations induced by HFD

Mice fed an HFD diet supplemented with 2′FL showed significantly lower body weight and fat mass gain (subcutaneous, epididymal, visceral and brown adipose tissues) compared with mice fed HFD alone (figure 1A–E). This could not be explained by food intake or lean/muscle mass since there were no differences between HFD and HFD+2′FL groups (online supplemental figure 1A-C). Additionally, 2′FL supplementation reduced glucose intolerance, as evidenced by the shape of the glycaemia curve during the oral glucose tolerance test and by the lower insulin levels in fasting state (figure 1F–I). These effects coincide with changes in hormones involved in metabolic pathways, since 2′FL significantly increased the concentration of glucagon-like peptide-1 (GLP-1) and peptide YY (PYY) and decreased leptin and glucagon (for the latter not significantly) while ghrelin was significantly reduced by the HFD, with no effects of 2′FL (figure 1J–N).

2′FL increases intestinal cells proliferation and markers involved in gut barrier function

2′FL supplementation significantly increased full caecum and its content weight by about 80% and 150% compared with control and HFD, respectively (figure 2A–C). 2′FL supplementation also increased the length of the jejunum by almost 15% compared with CT and HFD (figure 2D).

Analysing the expression of genes involved in gut barrier function by qPCR, we found that 2′FL significantly increased the antimicrobial peptides *Lyz1* and *Reg3g* in the caecum, and *proglucagon* in the caecum and colon while it induced the expression of *Reg3g* in the jejunum and colon, *Pla2g2a* in the colon and *intectin* in the ileum, without reaching significance (figure 2E–J).

2′FL affects GCs differentiation and mucus production and secretion

We next determined whether the effects of 2′FL supplementation on metabolism and gut barrier function were linked to changes in intestinal mucus. We showed that 2′FL significantly affected the expression of genes involved in GCs differentiation at different sites, with increased expression of *Elf3* in caecum and *Hes1* in colon, and decreased *Math1* and *Spdef* in caecum (figure 3A–E). In order to determine if the mucus inside the GCs was affected by the dietary treatments, we measured the proportion of the blue area (representing the mucins) over the total mucosal area, in histological sections using an Alcian blue staining. We found 22% more blue area in HFD+2′FL compared with HFD, though this difference did not reach significance (figure 3F,G).

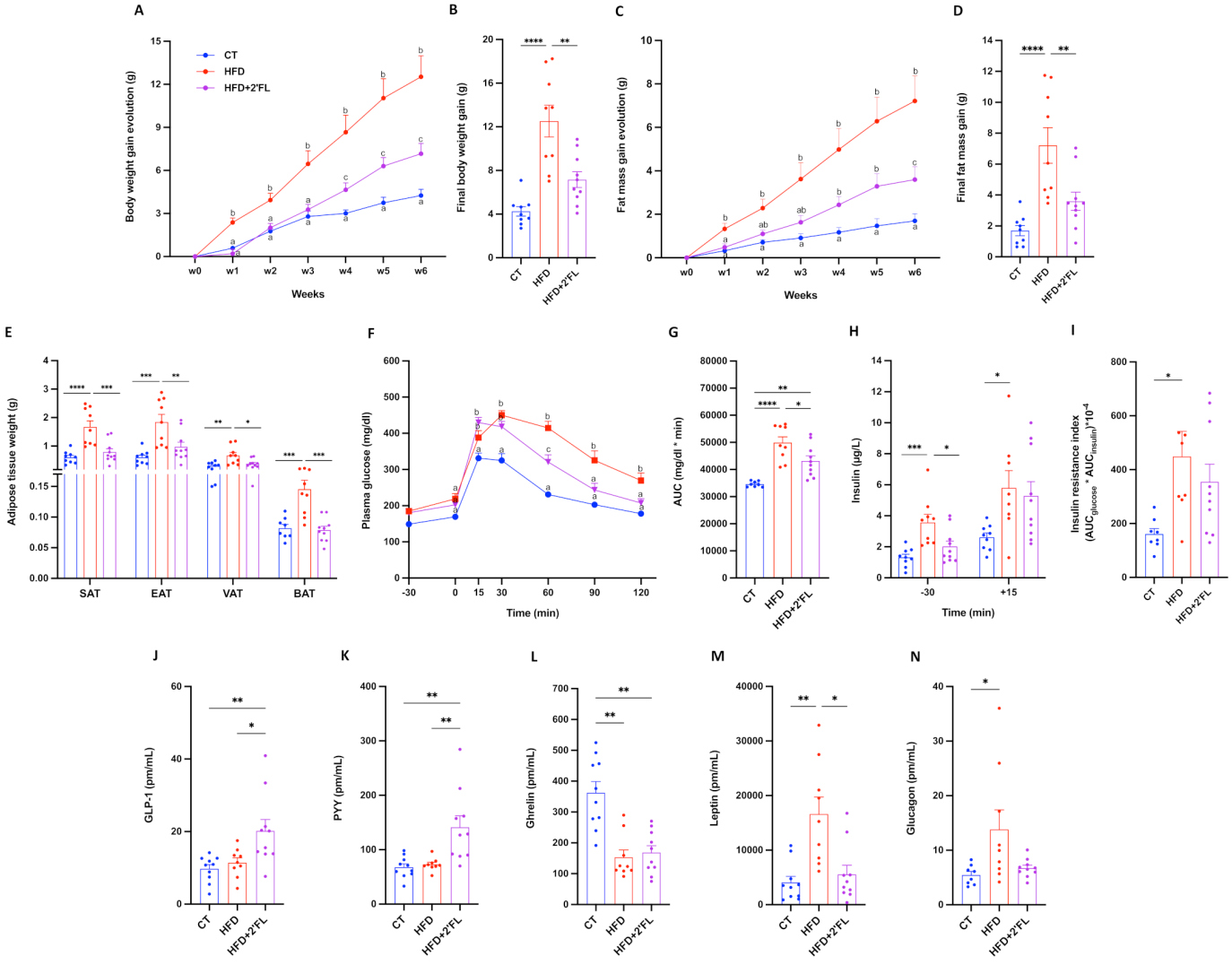

Figure 1 2'FL supplementation counteracts diet-induced obesity and glucose intolerance. (A) Body weight gain evolution and (C) fat mass gain evolution. (B) Final body weight gain and (D) fat mass gain. (E) Adipose tissue weights of subcutaneous (SAT), epididymal (EAT), visceral (VAT) and brown (BAT) adipose tissue. (F) Plasma glucose (mg/dL) profile before and after 2 g/kg of glucose oral challenge measured during the oral glucose tolerance test (OGTT) and (G) the mean area under the curve (AUC) (mg/dL×min). (H) Plasma insulin (µg/L) measured 30 min before and 15 min after the glucose administration during the OGTT. (I) Insulin resistance index determined by multiplying the area under the curve (from −30 to 15 min) of blood glucose and plasma insulin obtained during the OGTT. (J–N) Plasma levels from the portal vein of glucagon-like peptide-1 (GLP-1), peptide YY (PYY), ghrelin, leptin and glucagon. Data are means±SEM (n=7–10/group). One-way ANOVA followed by Tukey post hoc test was applied to figure B, D, E, G–K, N while Kruskal-Wallis followed by Dunn's test was applied to figure L,M, based on data distribution. Two-way ANOVA followed by Tukey post hoc test was applied to figure A, C, F. Data with different subscript letters are significantly different ($p<0.05$). *p<0.05; **p<0.01; ***p<0.001; ****p<0.0001. 2'FL, 2'-fucosyllactose; ANOVA, analysis of variance; HFD, high-fat diet.

Next, we set out to assess whether 2'FL treatment impacts intestinal mucins. We found that 2'FL significantly affected *Agr2* expression, required for the post-transcriptional synthesis and secretion of Muc2, which was decreased in caecum and increased in colon. In accordance with this observation, we also found a significant increase in *Muc2* expression (figure 3H,I). With regard to transmembrane mucins, 2'FL supplementation led to increased *Muc4* in jejunum, caecum and colon, *Muc13* in jejunum and caecum, and *Muc17* in caecum and colon (figure 3J–M). Furthermore, *Muc1* and *Muc13* expressions in the colon were negatively correlated with body weight and fat mass gain (online supplemental figure 2A,B).

Finally, we observed that dietary treatments differentially affected the expression of genes involved in intestinal mucus secretion and stabilisation. In particular, 2'FL supplementation tended to increase *Retnlb* in jejunum but decreased in the other intestinal segments. 2'FL supplementation increased two other key markers, *Nlrp6* in caecum and colon and *Fcgbp* in colon while slightly counteracting the effects of the HFD on the expression of *Atg5* and *Atg7* (figure 4A–E).

Although there was no difference in mucus thickness as assessed on histological sections (figure 4G,H), we found a significant higher weight of the mucus collected by scraping the colon in mice supplemented with 2'FL, suggesting a potential increase in mucus production (figure 4F).

Using a fluorescence in situ hybridisation (FISH) approach against 16S RNA to detect bacteria combined with a Muc2C3-specific staining of the mucus on colon sections, we observed an abrupt change from the inner to outer mucus layer with bacterial concentrations jumping from almost virtually free of bacteria to

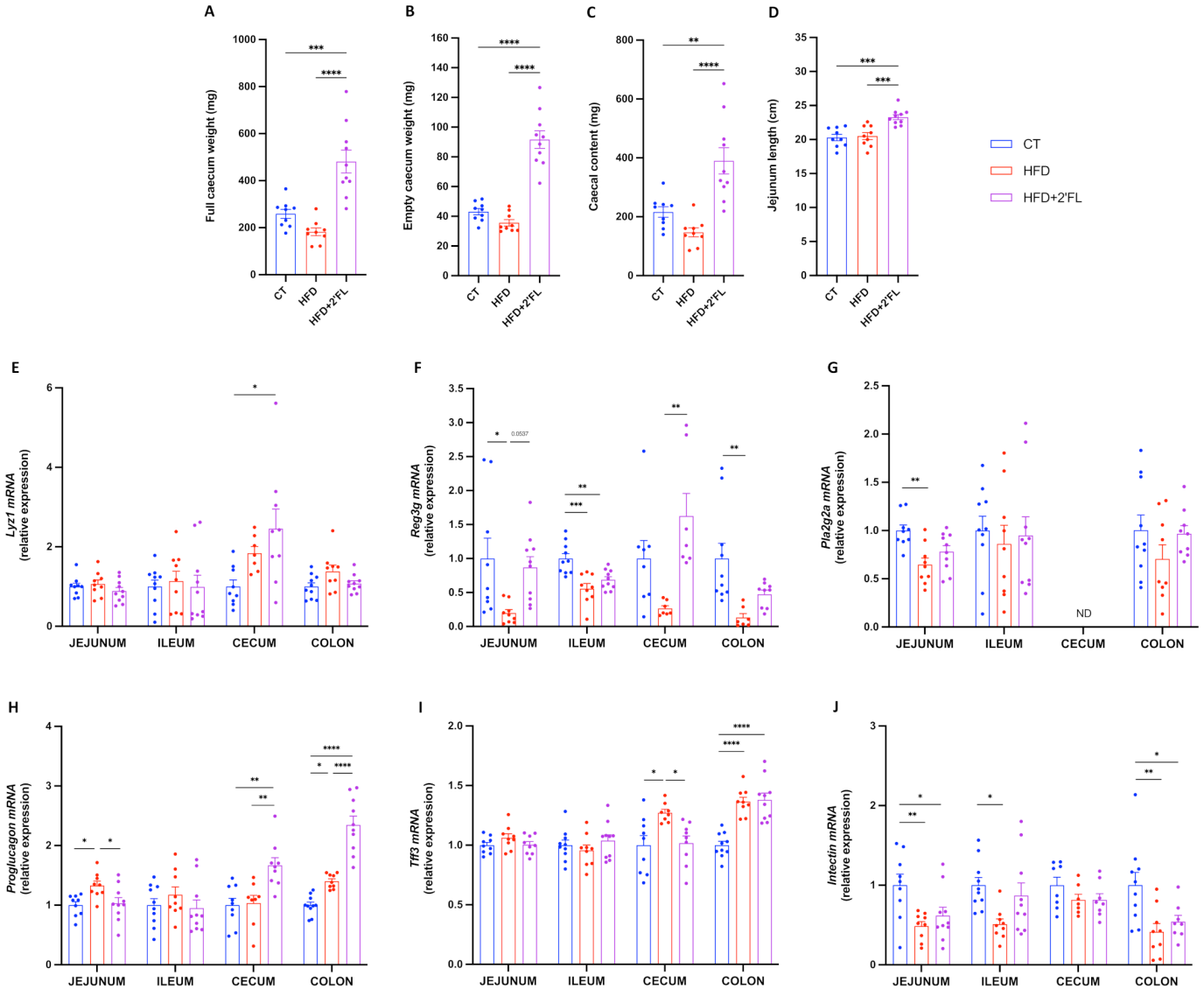

Figure 2 2'FL increases microbiota fermentation, intestinal cell proliferation and markers of the gut barrier. (A) Full caecum, (B) empty caecum and (C) caecal content weight. (D) Jejunum length. (E–J) mRNA relative expression of markers of the gut barrier function measured in the jejunum, ileum, caecum and colon. Antimicrobial peptides mRNA expression: (E) Lysozyme C (*Lyz1*), (F) Regenerating islet-derived 3-gamma (*Reg3g*), (G) Phospholipase A2 group II (*Pla2g2a*); (H) *Proglucagon*; (I) Trefoil factor 3 (*Tff3*); (J) *Intectin*. Data are means±SEM (n=7–12/group). Data were analysed using one-way ANOVA followed by Tukey post hoc test. *p<0.05; **p<0.01; ***p<0.001; ****p<0.0001. 2'FL, 2'-fucosyllactose; ANOVA, analysis of variance; ND, not detectable.

a high density without any perceptible gradient. The bacterial front was found to be morphologically intact in all groups. The thickness of the bacteria-free mucus was not statistically different between CT and HFD groups, though we observed a significant increase in the 2'FL treated group compared with the control group (p=0,01 Kruskal-Wallis test) (figure 5A).

When focusing on the apparent virtually free of bacteria inner mucus layer, we found that some bacteria, though very few, were able to penetrate it. We quantified the density by counting these cells and normalising to the area of mucus, but we found no differences between groups (figure 5B).

2'FL affects mucin glycan profile

To determine whether HFD and 2'FL supplementation affected mucin glycosylation, we first measured the expression of glycosyltransferases involved in elongation, branching and termination of the mucin glycan chain. We found that 2'FL significantly increased *Gcnt4*, *B3gnt6* and *C1galt1* in colon, *C1galt1c1* in caecum and colon, *Fut1* in jejunum and colon, *Fut8* and *St3gal1* in colon, *St3gal3* in jejunum and colon and *St3gal6* in colon (figure 6A–M). Interestingly, *Fut2* was decreased by the HFD in caecum and colon, but not affected by 2'FL supplementation. All the data from the mRNA expression described in the colon are schematised in figure 7.

We next analysed mucin glycosylation by tandem mass spectrometry (MS/MS) and found that two of them were significantly higher in HFD, compared with the CT and/or HFD+2'FL group (figure 8A–D). Figure 8E shows that 10 glycans were present in all the mice, 8 had a lower prevalence in the HFD group only or were restored following supplementation with 2'FL, and 3 were less prevalent in the HFD+2'FL group.

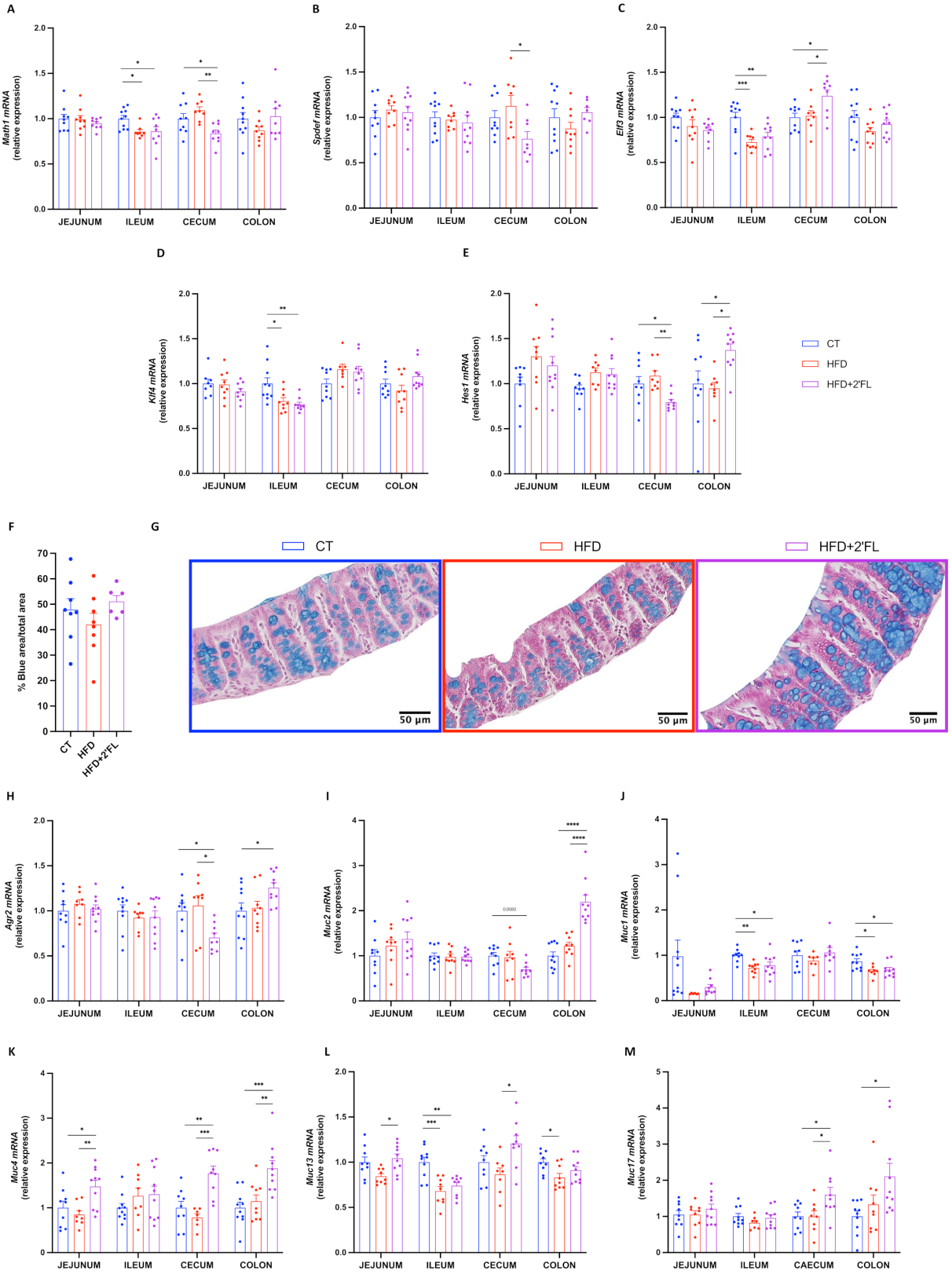

Figure 3 2'FL supplementation impacts on goblet cells and mucins production. (A–E) mRNA relative expression of transcriptional factors involved in the goblet cells differentiation, in the jejunum, ileum, caecum and colon: (A) atonal bHLH transcription factor 1 (*Math1*), (B) SAM pointed domain containing ETS transcription factor (*Spdef*), (C) E74 like ETS transcription factor 3 (*Elf3*), (D) kruppel like factor 4 (*Klf4*), hes family basic helix-loop-helix (bHLH) transcription factor 1 (*Hes1*). (F) Percentage of blue area on the total mucosal area in the proximal colon and (G) representative images for each group. (H–M) mRNA relative expression of markers involved in mucin production, in the jejunum, ileum, caecum and colon: (H) anterior gradient 2 (*Agr2*), (I) mucin 2 (*Muc2*), (J–M) mucin 1/4/13/17 (*Muc1*, *Muc4*, *Muc13, Muc17*). Data are means±SEM (n=6–12/group). One-way ANOVA followed by Tukey post hoc test or Kruskal-Wallis followed by Dunn's test were applied based on data distribution. *p<0.05; **p<0.01; ***p<0.001; ****p<0.0001. 2'FL, 2'-fucosyllactose; ANOVA, analysis of variance; HFD, high-fat diet.

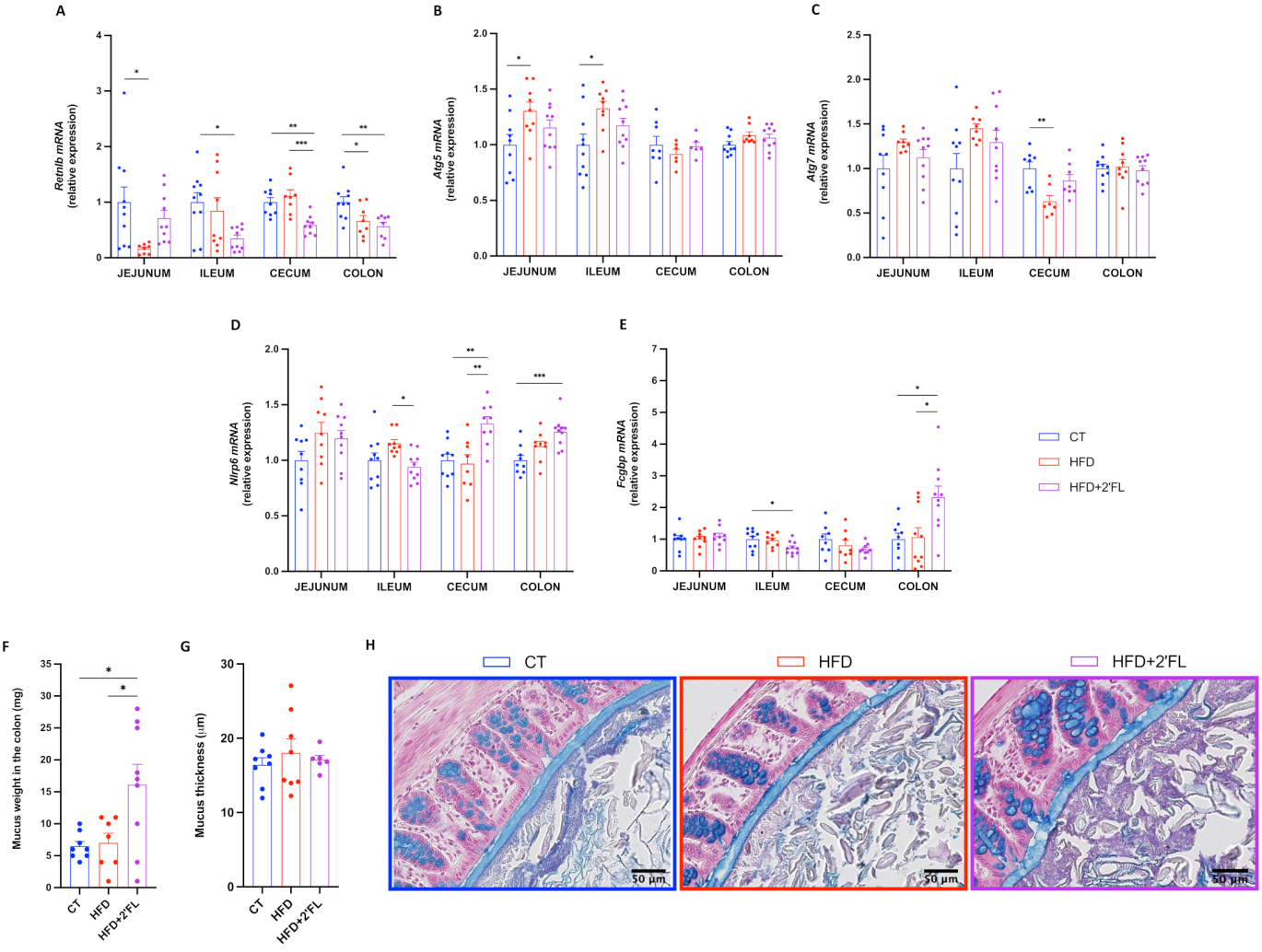

Figure 4 2′FL increases markers of mucus secretion. (A–E) mRNA relative expression of markers involved in the secretion of the mucus layer: (A) resistin-like beta (*Retnlb*), (B) autophagy protein 5 (*Atg5*), (C) autophagy protein 7 (*Atg7*), (D) NOD-like receptor family pyrin domain containing 6 (*Nlrp6*), (E) Fc gamma binding protein (*Fcgbp*). (F) Weight of the mucus in the colon after scraping in milligrams. (G) Mucus thickness in the proximal colon measured by ImageJ (in micrometre) and (H) representative images for each group. Data are means±SEM (n=6–12/group). One-way ANOVA followed by Tukey post hoc test or Kruskal-Wallis followed by Dunn's test were applied based on data distribution. *p<0.05, **p<0.01, ***p<0.001. 2′FL, 2′-fucosyllactose; ANOVA, analysis of variance; HFD, high-fat diet.

2′FL affects the endocannabinoid system

We previously discovered that different bioactive lipids belonging to the eCB system are able to exert control over the gut microbiota and the gut barrier function.[2 24–27] Hence, we measured caecal levels of eCBs (arachidonoylglycerol (AG) and anandamide (NAE 20:4)) and related *N*-acylethanolamines, and found that HFD+2′FL mice had significant lower levels of NAEs (16:1, 18:3, 20:0), LEA, OEA, PEA, DHEA and HEA, compared with CT and/or HFD mice. While, they had significant higher levels of mono-oleoylglycerol (OG) and mono-palmitoylglycerol (PG) (figure 9A). 2′FL affected the expression of genes involved in the biosynthesis and degradation of eCBs, by significantly upregulating *Daglb* and *Abdh6*, and downregulating *Abdh4*, *Faah* and *Mgl* (figure 9B).

2′FL changes gut microbiota composition

Before the treatment all mice shared a similar faecal microbiota composition, while in the end both the faecal and caecal microbiota profiles were significantly clustered based on the diets (figure 10A–C). The results shown below refer to changes observed in both relative and absolute abundance.

At the phylum level, the caecal gut microbiota of CT and HFD groups was dominated by Desulfobacterota while HFD+2′FL by Bacteroidota and Verrucomicrobiota. In the faeces, the CT group was dominated by Bacteroidota, HFD by Desulfobacterota and HFD+2′FL by Bacteroidota and Verrucomicrobiota (online supplemental figure 3A–D and online supplemental tables 1 and 2).

At the genus level, the caecal gut microbiota was enriched in uncultured *Desulfovibrionaceae* in the CT and HFD groups (35.1 and 51.7%, respectively), whereas *Akkermansia* and *Bacteroides* were the dominant genera in the HFD+2′FL group (39% and 24.8%, respectively) (figure 10D,E). Similarly, the faecal gut microbiota was dominated by uncultured *Desulfovibrionaceae*, *Rikenellaceae* RC9 gut group and *Akkermansia* in the CT group (19.4%, 17.3% and 18.4%, respectively), by uncultured *Desulfovibrionaceae* in the HFD group (38.8%), and *Bacteroides* and *Akkermansia* in the HFD+2′FL group (37.1% and 29.8%, respectively) (figure 10F,G) .

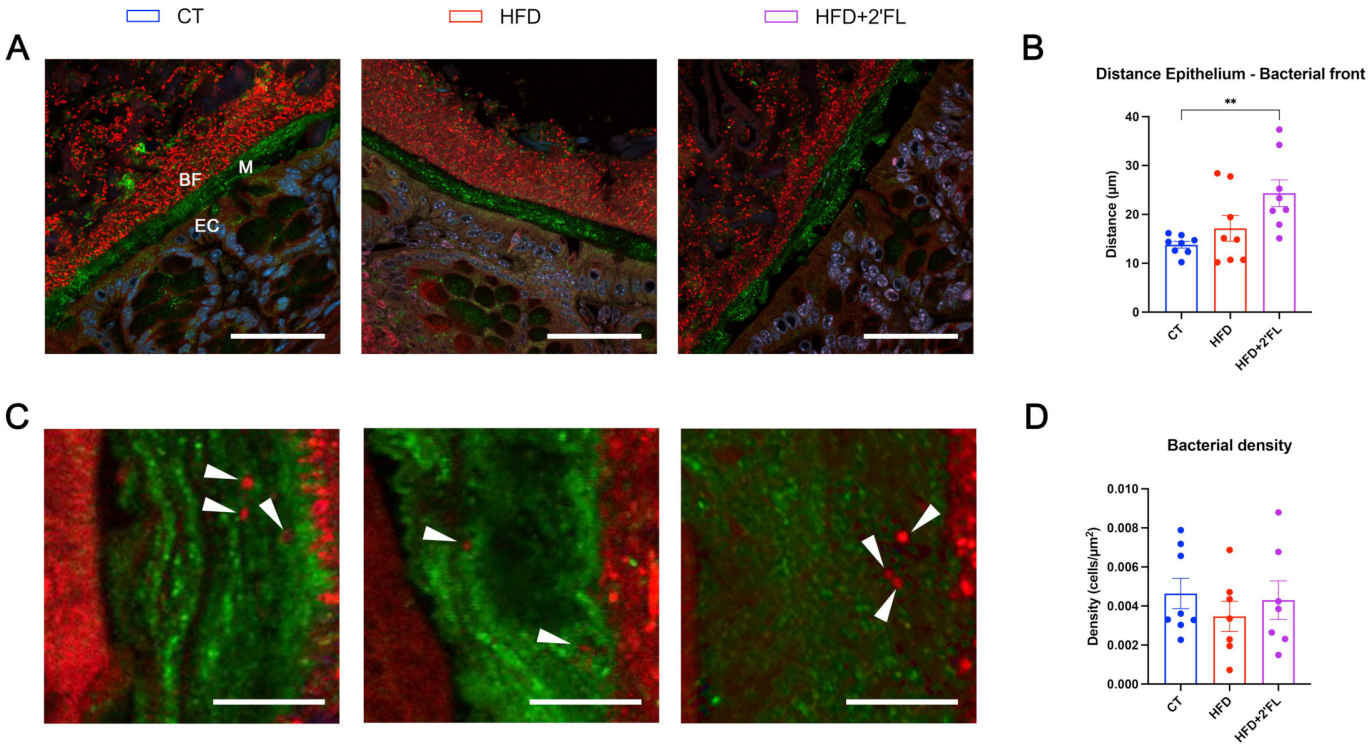

Figure 5 Pictures representative of the bacterial penetration assessed by measuring the distance between the bacterial front and the epithelial cells (A, B) and the bacterial density in the inner mucus layer (C, D). (A) Mouse distal colon section in which Muc2C3 immunostaining shows the Muc2-positive mucus layer on the epithelium. The inner mucus layer (M) is almost completely devoid of bacteria, which are visualised by a FISH approach using a general bacterial probe conjugated with C3 (red), whereas the outer mucus layer contains large concentrations of bacteria with a clearly delineated bacterial front (BF). The sections are counterstained with DAPI to visualise nuclei (blue). Epithelial cells (EC) emit some autofluorescence making them visible (Scale bar: 50 µm). (B) Quantitative measurement of the spatial separation between the epithelial cells and the bacterial front. (C) Magnification (×20) of the inner mucus layer and of penetrating bacteria. Epithelial cells are on the left, while the bacterial front is on the right (scale bar: 10 µm). (D) Quantification of the bacterial density in the inner mucus layer (number of bacterial cells counted divided by the surface area of mucus). Data are means±SEM (n=7–8/group). Arrow heads show bacteria in red. Data were analysed using Kruskal-Wallis test followed by Dunn's test. **p<0.01. FISH, fluorescence in situ hybridisation; HFD, high-fat diet.

Notably, HFD-fed mice had significant lower levels of *Akkermansia*, *Parasutterella*, unclassified *Tannerellaceae*, *Muribaculaceae* and *Rikenellaceae* RC9 gut group compared with CT mice while 2'FL treatment significantly increased *Akkermansia*, *Parasutterella*, unclassified *Tannerellaceae* and *Bacteroides* compared with HFD only, in the faeces (figure 11A–C, online supplemental table 3).

2'FL affects bacterial glycosidases and faecal proteome

To evaluate the mucus degradation by the gut microbiota, we investigated bacterial GHs alpha-L-fucosidase and alpha-D-galactosidase by in-gel fluorescent activity-based probes (ABP) labelling.[28 29] We found ABP-labelling for alpha-L-fucosidase only in the HFD+2'FL group, with mice within this group displaying different profiles. While, alpha-D-galactosidase labelling was present in CT and HFD+2'FL, without any signals in HFD (figure 12A).

To further confirm the presence of GHs, we analysed the total faecal proteome, using a bespoke database containing mouse proteins and GHs involved in mucin glycan degradation: fucosidases, galactosidases, hexosaminidases and sialidases. The principal component analysis (PCA) showed different clustering between HFD and HFD+2'FL (figure 12B–D). Particularly, when taking only GHs into account, CT and HFD displayed overlapping clusters, while HFD+2'FL cluster was completely separated. The volcano plot showed that HFD feeding significantly changed the abundance of 17 proteins, while 2'FL supplementation changed 12 proteins compared with CT and 30 compared with HFD (figure 12E–G).

Interestingly, 2'FL supplementation significantly upregulated beta-galactosidase, alpha-L-fucosidase, beta-hexosaminidase and beta-*N*-acetylhexosaminidase, belonging to *Bacteroidales* and *Lachnospiraceae* bacterial families (figure 13A–H).

In addition to changes in GHs, dietary treatments affected several faecal mucins. Indeed, Muc2 was significantly lower in HFD and HFD+2'FL groups compared with the CT group, and Muc13 and Muc17 were significantly lower in HFD+2'FL compared with CT; while Muc5ac was significantly higher in HFD+2'FL compared with HFD (figure 13I–L).

Taking into account the results from the Wilcoxon rank-sum test, we found that HFD significantly changed 78 proteins compared with CT, while supplementing 2'FL changed 90 proteins compared with HFD (online supplemental table 4).

By executing KEGG pathway enrichment of mouse proteins, we observed that HFD feeding significantly upregulated proteins involved in protein digestion and absorption while it significantly downregulated proteins involved in carbon metabolism, biosynthesis of amino acids, metabolic pathways, fat digestion and absorption, and others (figure 14A). Notably, 2'FL supplementation reversed all the changes induced by HFD (figure 14B, online supplemental figure 4).

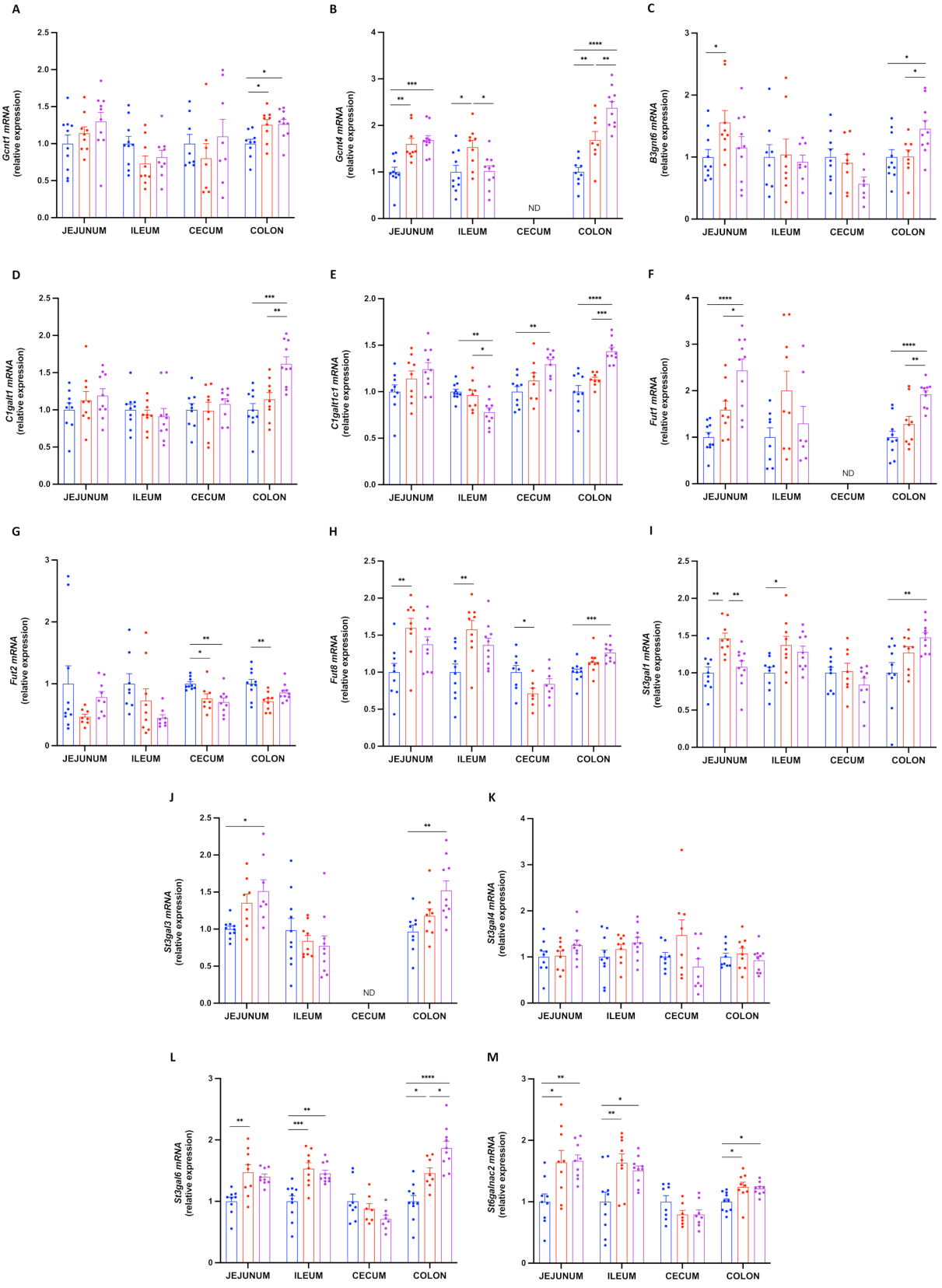

Figure 6 2′FL increases the expression of glycosyltransferases involved in mucin glycosylation. mRNA relative expression of glycosyltransferases in the jejunum, ileum, caecum and colon: (A) glucosaminyl (*N*-acetyl) transferase 1 (*Gcnt1*), (B) glucosaminyl (*N*-acetyl) transferase 4 (*Gcnt4*), (C) UDP-GlcNAc:betaGal beta-1,3-*N*-acetylglucosaminyltransferase 6 (*B3gnt6*), (D) core one synthase, glycoprotein-*N*-acetylgalactosamine 3-beta-galactosyltransferase 1 (*C1galt1*), (E) C1GALT1 specific chaperone 1 (*C1galt1c1*), (F–H) fucosyltransferase 1/2/8 (*Fut1*, *Fut2*, *Fut8*), (I–M) ST3 b-galactoside a-2,3-sialyltransferase 1/3/4/6 (*St3gal1*, *St3gal3*, *St4gal4*, *St3gal6*), (O) ST6 *N*-acetylgalactosaminide a-2,6-sialyltransferase 2 (*St6galnac2*). Data are means±SEM. (n=7–12/group). Data were analysed using one-way ANOVA followed by Tukey post hoc test. *p<0.05; **p<0.01; ***p<0.001; ****p<0.0001. 2′FL, 2′-fucosyllactose; ANOVA, analysis of variance; ND, not detectable.

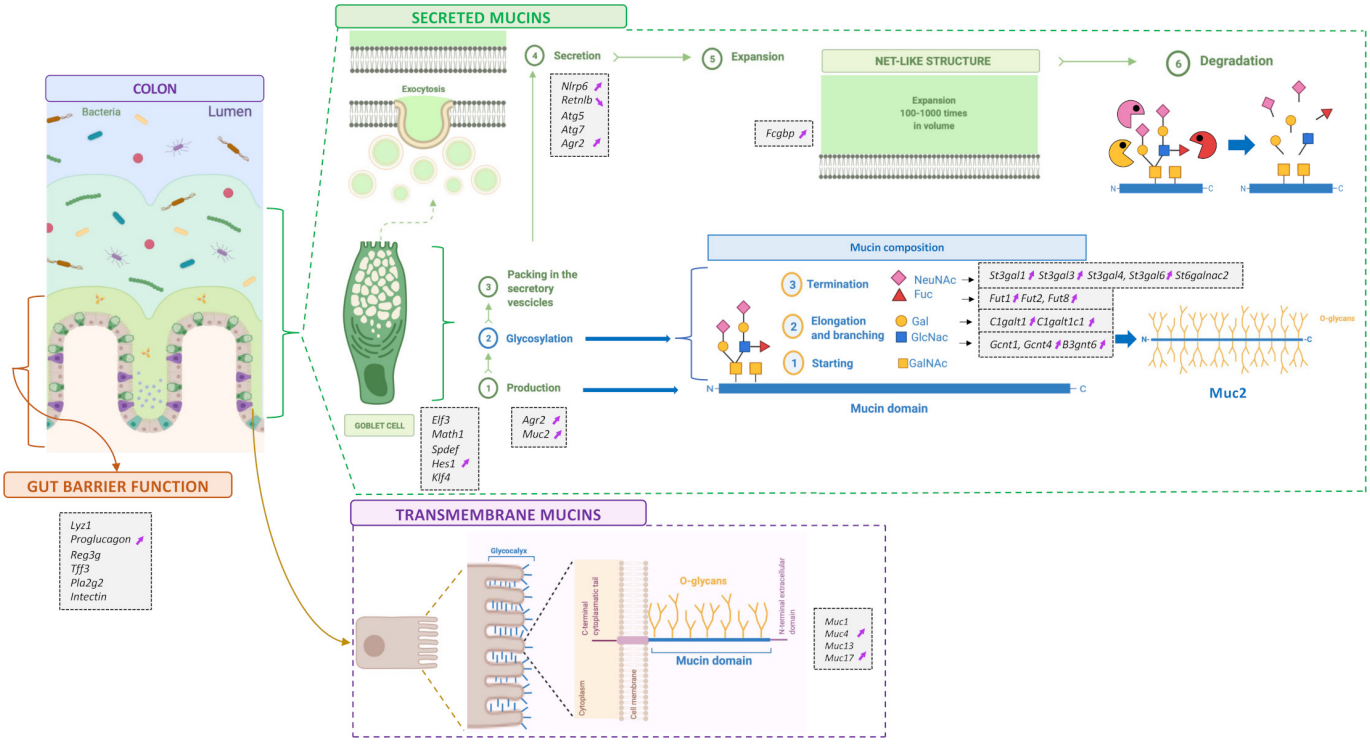

Figure 7 Schematic figure summarising the expression analysis of 35 genes in the jejunum, ileum, caecum and colon. Markers involved in gut barrier function and mucins production, glycosylation and secretion measured by RT-qPCR. Markers are enclosed in small grey boxes. Purple arrows indicate those that significantly changed due to 2′FL supplementation in the colon. 2′FL, 2′-fucosyllactose.

Humans proteomic

The results observed in rodents let us wondering if similar changes could be found in humans. We analysed the faecal proteome of lean and obese subjects and found that, among 133 proteins, 17 were significantly changed and increased in obese subjects (figure 15A; online supplemental tables 5 and 6). By doing functional annotation clustering, we observed that these proteins were linked to the enrichment of terms that were also enriched in HFD-fed mice (online supplemental figure 5, online supplemental table 7). Interestingly, by investigating the molecular function, biological process, KEGG pathway and disease, we found that they were involved in metabolic processes and diseases, such as type 2 diabetes (figure 15B, online supplemental table 8).

MATERIAL AND METHODS

See online supplemental materials and methods.

DISCUSSION

In this study, we found that 2′FL counteracted diet-induced obesity and metabolic alterations together with affecting mucus production, secretion and glycosylation, as well as gut microbiota composition, bacterial GHs, faecal proteome and eCB system.

Previous studies showed that 2′FL reduced energy intake, body weight or fat mass, in mice fed HFD, without affecting plasma glucose.[20 21] Here, we found that HFD-fed mice supplemented with 2′FL had significantly lower body weight gain, fat mass gain, plasma glucose and insulin levels. These effects could partially be explained by a change in different hormones involved in appetite regulation and energy metabolism. Indeed, GLP-1 and PYY were significantly higher and leptin and glucagon were significantly lower in mice supplemented with 2′FL.

HFD feeding and obesity have been associated with gut barrier disruption, increased lipopolysaccharide translocation and metabolic endotoxaemia.[1] Supplementing 2′FL to HFD has shown protective effects on markers of the gut barrier, but the mechanisms were not explored.[20 21] In this study 2′FL supplementation led to higher expression of antimicrobial peptides *Lyz1* and *Reg3g*, and *proglucagon*, the precursor of GLP-1 and GLP-2, involved in improved gut barrier function, in specific sites of the gastrointestinal tract.

To further explore the mechanisms involved in gut barrier regulation, we focused on the mucus layer. In vitro studies reported that 2′FL led to enhanced *MUC2* expression and secretion on human GCs during inflammatory conditions.[23 30] While, in vivo, 2′FL ameliorated colitis by recovering GC numbers and improving *Muc2* expression in mice.[22 23] However, no studies investigated the effect of 2′FL supplementation on the intestinal mucus in the context of HFD feeding and obesity. Our data showed that 2′FL supplementation led to increased expression of several markers involved in GCs differentiation (eg, *Elf3* and *Hes1*) and synthesis and secretion of the main component of the mucus layer (ie, *Agr2*, *Muc2*). In addition, several markers related to mucus secretion and stabilisation were also increased (eg, *Retnlb*, *Nlrp6* and *Fcgbp*). These effects were linked to a higher quantity of mucus collected in the colon of mice receiving 2′FL, and with GCs more filled with mucus. The mucus penetrability to bacteria assessed by two parameters (ie, the distance from the bacterial front to the epithelial cells and the density of bacterial cells within the inner mucus layer) did not show significant differences between CT and HFD groups, though we observed an increased mucus layer thickness in the 2′FL treated group compared with the CT, suggesting that 2′FL protects the epithelium against bacteria penetration.

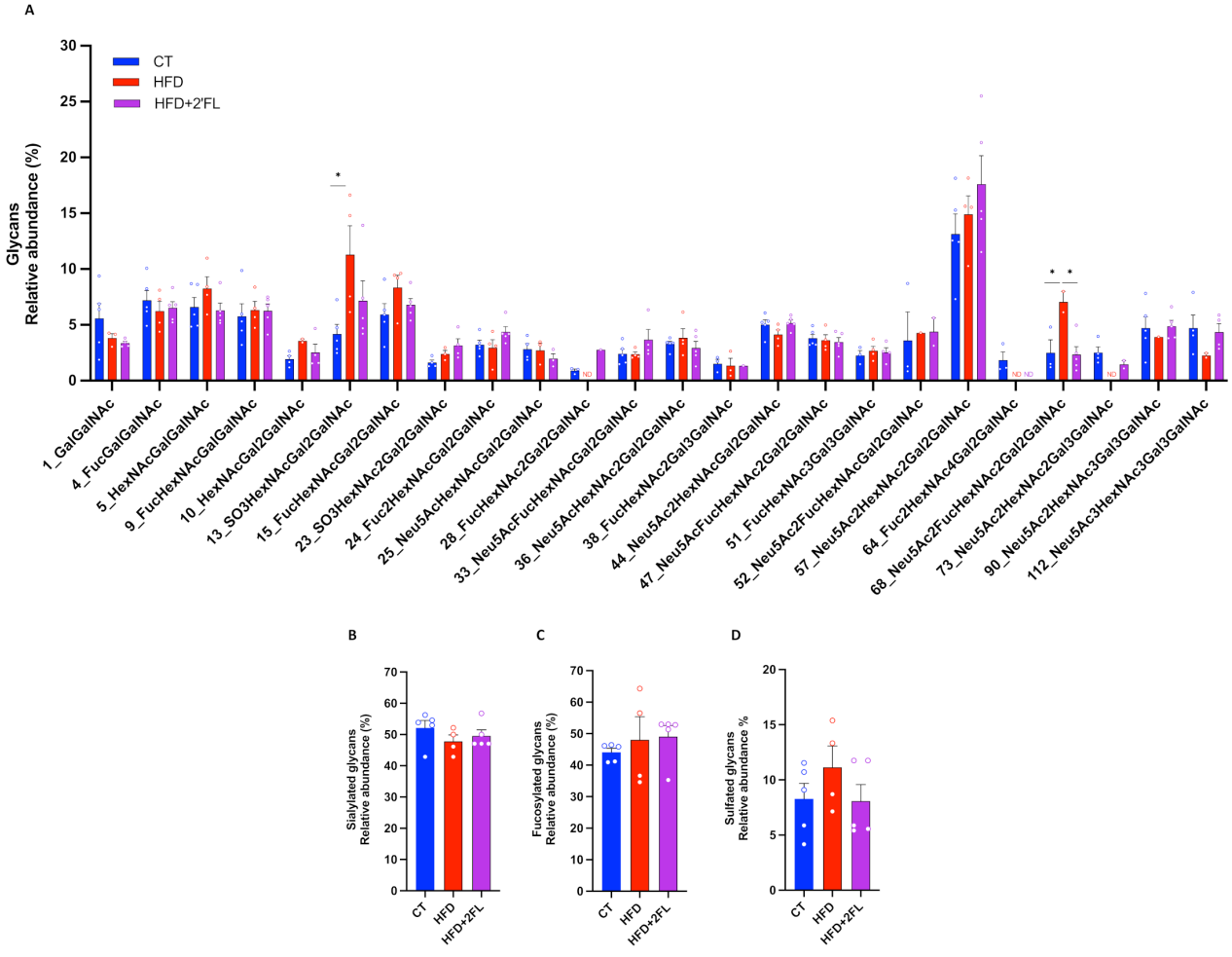

E

GLYCANS PREVALENCE				
Glycans	CT	HFD	HFD+2FL	Prevalence
FucGalGalNAc	100%	100%	100%	In all mice
HexNAcGalGalNAc	100%	100%	100%	
FucHexNAcGalGalNAc	100%	100%	100%	
SO3HexNAcGal2GalNAc	100%	100%	100%	
FucHexNAcGal2GalNAc	100%	100%	100%	
Fuc2HexNAcGal2GalNAc	100%	100%	100%	
Neu5AcHexNAc2Gal2GalNAc	100%	100%	100%	
Neu5Ac2HexNAcGal2GalNAc	100%	100%	100%	
Neu5AcFucHexNAc2Gal2GalNAc	100%	100%	100%	
Neu5Ac2HexNAc2Gal2GalNAc	100%	100%	100%	
Neu5Ac2HexNAc3Gal3GalNAc	100%	25%	100%	Restored/⬆ in HFD+2FL vs HFD
HexNAcGal2GalNAc	80%	50%	80%	
SO3HexNAc2Gal2GalNAc	80%	75%	80%	
Neu5Ac3HexNAc3Gal3GalNAc	80%	50%	80%	
GalGalNAc	100%	75%	80%	
Neu5Ac2FucHexNAcGal2GalNAc	60%	25%	40%	
Neu5Ac2HexNAc2Gal3GalNAc	80%	0%	40%	
FucHexNAc2Gal2GalNAc	60%	0%	20%	
Neu5Ac2FucHexNAc2Gal2GalNAc	60%	50%	100%	⬆ HFD+2FL
Neu5AcFucHexNAcGal2GalNAc	100%	100%	80%	⬇ HFD+2FL
Neu5AcHexNAcGal2GalNAc	80%	75%	60%	
FucHexNAc2Gal3GalNAc	60%	75%	20%	
FucHexNAc3Gal3GalNAc	60%	100%	80%	⬆ HFD
Fuc2HexNAc4Gal2GalNAc	60%	0%	0%	Only in CT

Figure 8 High-fat diet and 2'FL supplementation affects mucin glycans composition in the colon. (A) Glycan relative abundance in percentage; relative abundance of (B) sialylated glycans, (C) fucosylated glycans and (D) sulfated glycans. (E) Glycan prevalence calculated by dividing the number of mice for which the glycan was present for the total number of mice in the group. Only glycans present in at least 3 mice and in at least one group are shown. Data are means±SEM (n=4–5/group). Data were analysed using Kruskal-Wallis followed by Dunn's test. *p<0.05. 2'FL, 2'-fucosyllactose; HFD, high-fat diet; ND, not detectable.

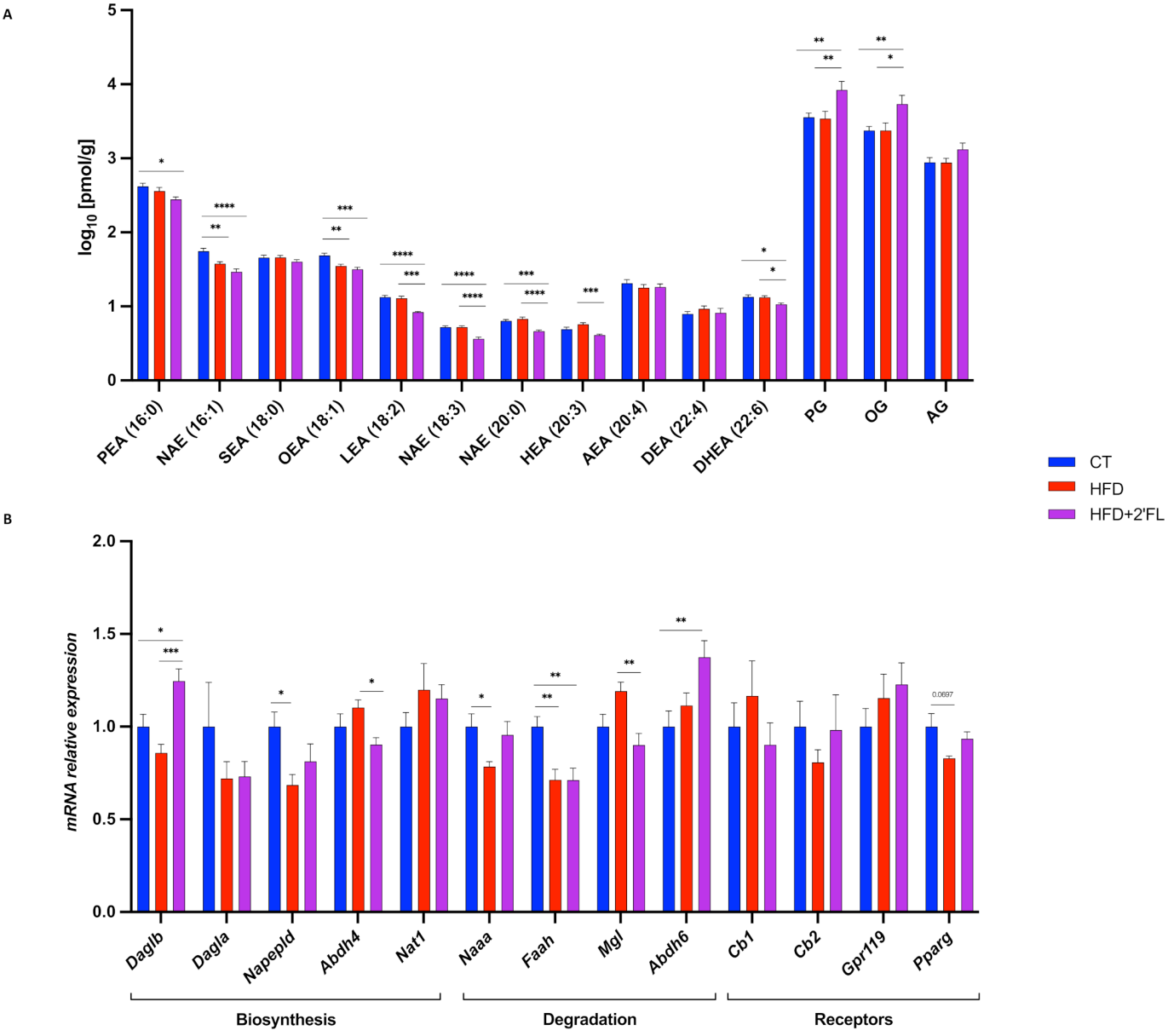

Figure 9 Different caecal eCBome tone in 2′FL supplemented mice. (A) Concentrations of the eCBome-related mediators in the caecal tissue (pmol/g wet tissue weight) measured by ultra-high-performance liquid chromatography–tandem mass spectrometry (UHPLC-MS/MS). (B) mRNA relative expression of receptors and metabolic enzymes for monoacylglycerols and *N*-acylethanolamines measured by RT-qPCR. Data are means±SEM (n=9–10/group). Data were analysed using one-way ANOVA followed by Tukey post hoc test. *p<0.05; **p<0.01; ***p<0.001; ****p<0.0001. 2′FL, 2′-fucosyllactose; Abdh4, alpha/beta-hydrolase 4; Abdh6, α/β-Hydrolase domain-containing 6; AEA, *N*-arachidonoylethanolamine; AG, 2-arachidonoylglycerol; ANOVA, analysis of variance; Cb1/Cb2, cannabinoid type 1/2 receptors; DEA, *N*-docosatetraenylethanolamine; Dagla, diacylglycerol lipase-alpha; Daglb, diacylglycerol lipase beta; DHEA, *N*-docosahexaenoylethanolamine; Faah, fatty-acid amide hydrolase; Gpr119, G-protein-coupled receptor 119; HEA, *N*-homo-linolenylethanolamine; LEA, *N*-linoleylethanolamine; Mgl, monoacylglycerol lipase; Naaa, *N*-acylethanolamine acid amidase; NAE, *N*-acylethanolamine; Napepld, N-acyl phosphatidylethanolamine phospholipase D; Nat1, N-acetyltransferase 1; OEA, *N*-oleoylethanolamine; OG, mono-oleoylglycerol; PEA, *N*-palmitoylethanolamine; PG, mono-palmitoylglycerol; Pparg, peroxisome proliferator-activated receptor gamma SEA, *N*-stearoylethanolamine.

In addition to the secreted mucins, other important components of the gut barrier are transmembrane mucins. We found that 2′FL supplementation significantly upregulated the expression of *Muc4*, *Muc13* and *Muc17* in different intestinal compartments. Interestingly, *Muc1* and *Muc13* expressions in the colon were negatively correlated with body weight and fat mass gain (online supplemental figure 2A,B), suggesting their potential involvement in metabolic processes. However, their role in the context of obesity and metabolic disorders is still unknown, as only a few studies focused on these aspects. Two studies showed that 2′FL impacted glycocalyx average thickness and increased mRNA levels of *Muc1* in the presence of *Escherichia coli* challenge.[31 32] To our knowledge, no other data on transmembrane mucins and 2′FL are available.

The composition of mucin glycans in the intestine has been shown to be important for microbial colonisation.[10] Glycosyltransferases are the enzymes responsible for mucin glycosylation and it has been suggested that they are affected by dietary

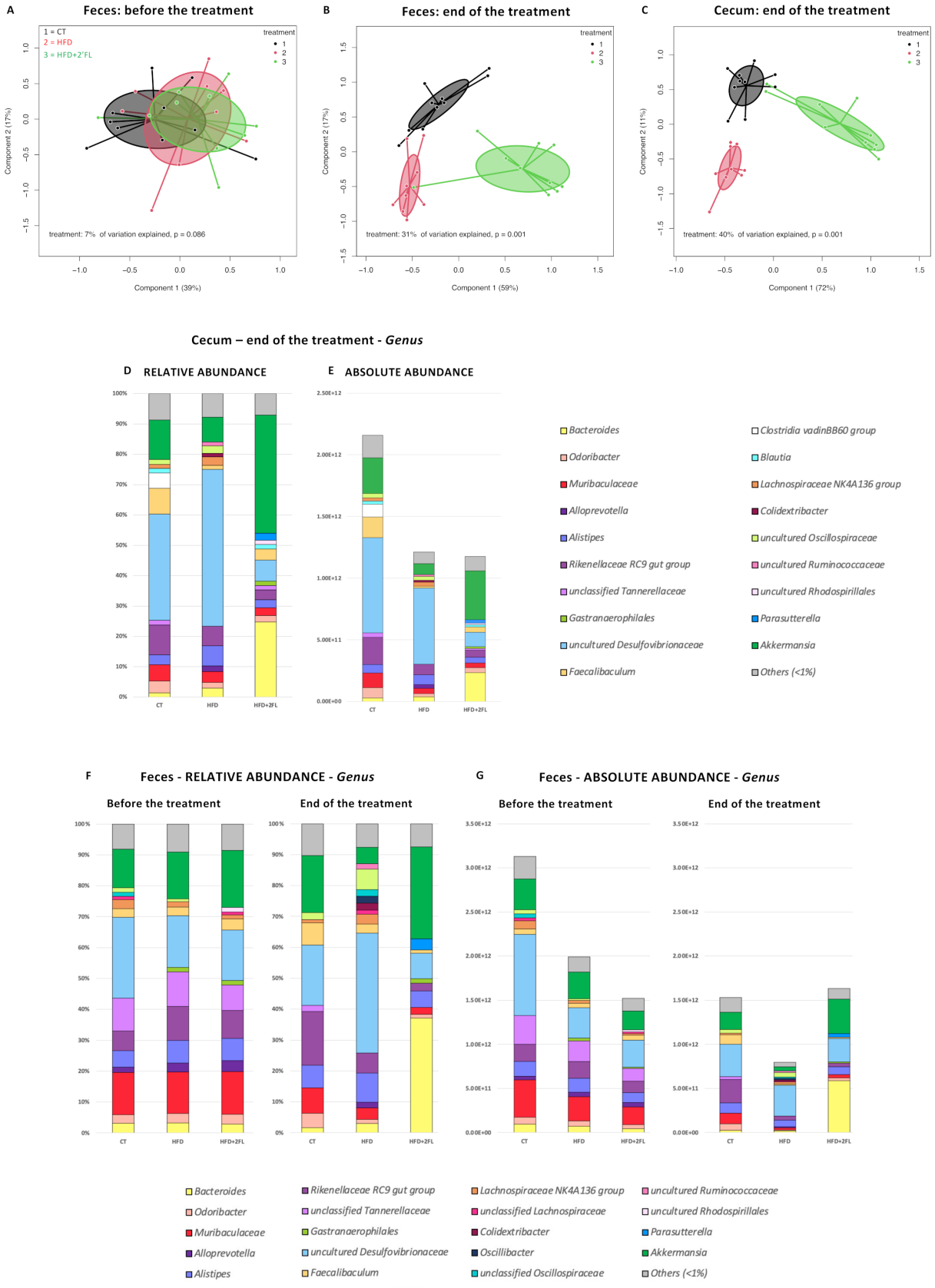

Figure 10 2'FL induces changes in the caecal and faecal gut microbiota composition. Principal coordinates analysis (PCoA) plot of the gut microbiota, in which mice are grouped by treatment, based on the Bray-Curtis dissimilarity in (A) faeces before the treatment (B) faeces at the end of the treatment and (C) caecum at the end of the treatment (n=9–10/group). (D–G) Bar graphs showing grouped taxonomic profiles of the gut bacteria at the genus level: (D, E) relative and absolute abundance in the caecum, at the end of the treatment; (F, G) relative and absolute abundance in the faeces, before and at the end of the treatment (n=9–10/group). Only the bacterial genera with >1% relative abundance are shown; the rest are indicated as 'others (<1%)'. 2'FL, 2'-fucosyllactose; HFD, high-fat diet.

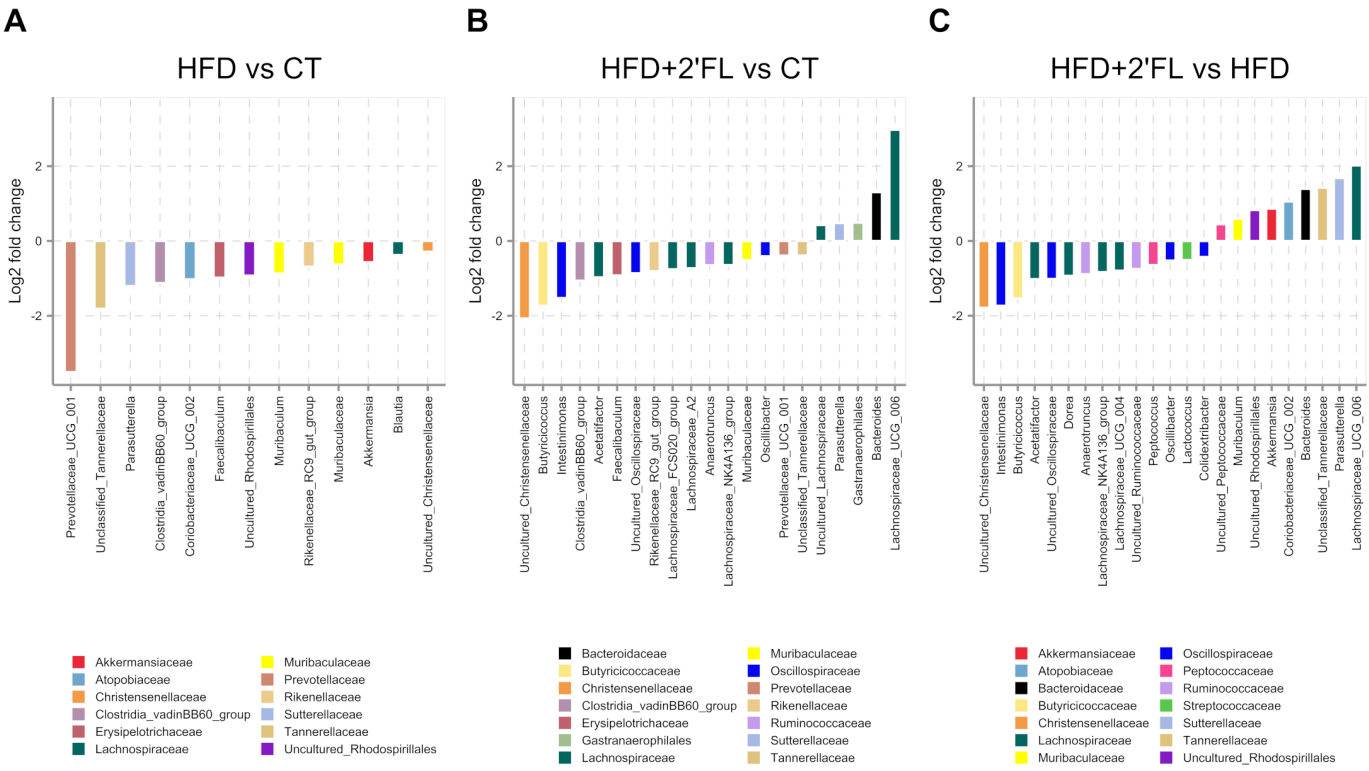

Figure 11 Bacterial genera significantly differed in absolute abundance (FDR-corrected p<0.05) in (A) HFD compared with CT (log2 fold change values calculated relative to CT), (B) HFD+2′FL compared with CT (log2 fold change values calculated relative to CT) and (C) HFD+2′FL compared with HFD (log2 fold change values calculated relative to HFD). Bar colour and bottom legend denote family-level taxonomic classification. See online supplemental table 3 for full results. 2′FL, 2′-fucosyllactose; HFD, high-fat diet.

treatments, which could impact Muc2 glycosylation.[33] Here, we found that 2′FL supplementation significantly affected the expression of glycosyltransferases, mainly in the colon where 9 out of 13 of them were upregulated. Such changes were also observed in a previous study following supplementation of mice with fructooligosaccharides.[34] Interestingly, we found that *Fut2* expression in the colon negatively correlated with body weight gain and fat mass gain (online supplemental figure 2C). Together with previous studies showing that *Fut2* mutation led to liver disease, these findings suggest that it could probably be involved in metabolic processes.[35 36]

Based on these results, we asked whether mucin glycan composition could be affected by dietary intervention. Previous studies showed that HFD alone altered mucin glycosylation, by increasing the sialo/sulfomucin ratio, altering lectin-binding pattern and overexpressing galβ1,3galnac terminal dimers.[5] Here, we observed that 2 out of 24 mucin glycans identified were significantly higher in HFD compared with the CT and/or HFD+2′FL groups while others did not reach statistical significance, probably due to the limited number of mice analysed. Notably, we found that among the 10 mucin glycans present in all mice, 8 had a lower prevalence only in HFD or were restored by 2′FL supplementation and 3 were less prevalent in the HFD+2′FL group. The 'restoration' of glycans prevalence by 2′FL suggests that the prebiotic treatment can be used to counteract alterations induced by HFD. In healthy humans, MUC2 O-glycosylation is uniform while it is altered in patients with active ulcerative colitis and associated with increased inflammation.[37 38] A different profile was also observed in human colon cancer, linked to tumour metastatic potential and poor prognosis.[39 40] Understanding the pattern of mucin glycosylation in patients with obesity and metabolic disorders, and how these could be modulated by nutritional treatments, could be useful in inducing the colonisation of specific bacteria associated with beneficial effects. To date, progress has been impeded by the scarcity of research in humans, which is hampered by the need for invasive methods such as biopsy collection.[41] Surprisingly, a recent study showed that the mucus structure on freshly excreted faecal pellets was identical to that of the faecal pellets in the corresponding colon tissue, suggesting that faecal-associated mucus may support noninvasive strategies for disease diagnosis in humans.[42]

In addition to proteins and enzymes, lipid mediators also play an important role in regulating energy homeostasis. Among them, the eCB system has been shown to regulate energy, glucose and lipid metabolism, gut barrier function and microbiota–host interactions.[43] Here, we found that mice receiving 2′FL had significantly lower levels of NAEs and decreased expression of *Abdh4* and *Mgl*. In contrast, mice receiving 2′FL showed increased levels of OG and PG compared with the CT and HFD groups. These bioactive lipids were previously reported to be significantly increased in the colon of mice and in the blood of obese humans treated with *Akkermansia muciniphila*, both exhibiting an improved gut barrier, lower inflammation and improved glucose metabolism.[2 44–46] In addition, mono-OG has been shown to stimulate GLP-1 secretion and improve glucose metabolism.[47] Short-chain fatty acids (SCFAs) have also been shown to stimulate the secretion of GLP-1 and PYY. However, we did not find any increase in butyrate, propionate and acetate in the caecal content but rather a significant decrease of several SCFAs and branched SCFA after 2′FL treatment (online supplemental figure 6). These findings indicate that 2′FL could affect the metabolism and the mucus layer by acting through the eCB system.

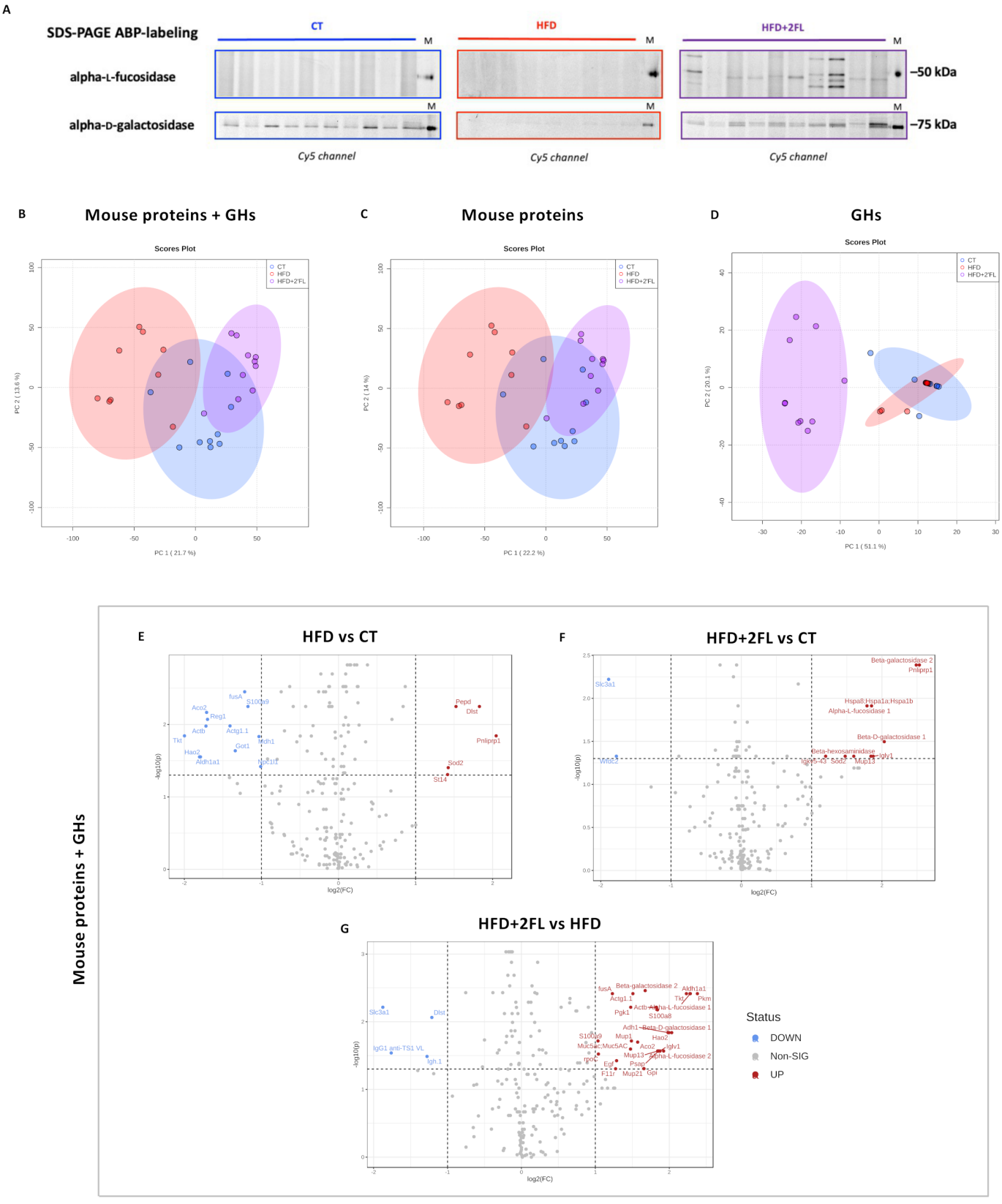

Figure 12 High-fat diet and 2′FL supplementation affects faecal proteome. (A) Cy5-ABP-labelling of alpha-L-fucosidase and alpha-D-galactosidase from mouse faecal extract (1 µg of proteins; 1 µM α-L-fucosidase and 0.5 µM α-galactosidase). Principal component analysis (PCA) of (B) faecal mouse proteins and GHs together, of (C) mouse proteins only and of (D) GHs separately. (E–G) Volcano plot comparing the different groups together, including mouse proteins and GHs. PCA and volcano plot were done with MetaboAnalyst (n=9–10/group). 2′FL, 2′-fucosyllactose; GHs, glycosyl hydrolases; HFD, high-fat diet.

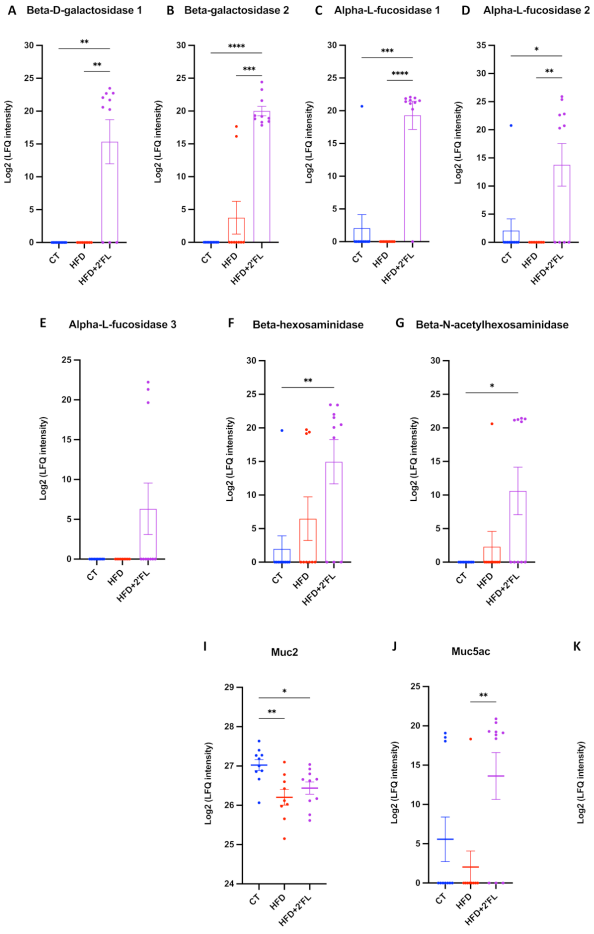

H

GHs: HFD+2FL vs HFD and CT

Protein name	Protein ID	Taxonomy (family)
Beta-D-galactosidase 1	A0A174R2Q3	Bacteroidales
	D7ID75	Bacteroidales
Beta-galactosidase 2	A0A7X5J262	Lachnospiraceae
	A0A3R8JS06	Lachnospiraceae
	A0A7G9FKZ3	Lachnospiraceae
	A0A356DQV3	Lachnospiraceae
	A0A3D4SAR0	Lachnospiraceae
Alpha-L-fucosidase 1	A0A3R8LD36	Lachnospiraceae
Alpha-L-fucosidase 2	R9JU09	Lachnospiraceae
	A0A7X5EID8	Lachnospiraceae
	A0A6L9GX20	Lachnospiraceae
Alpha-L-fucosidase 3	R9JU04	Lachnospiraceae
	A0A7X5IZK1	Lachnospiraceae
	A0A6L9GYJ9	Lachnospiraceae
	A0A2Y9BNB2	Lachnospiraceae
Beta-hexosaminidase	A0A351TFE7	Lachnospiraceae
	A0A6L9H1M8	Lachnospiraceae
Beta-N-acetylhexosaminidase	A0A7K3MF78	Bacteroidales
	A0A7J0A260	Bacteroidales
	A0A6H0KQS9	Bacteroidales
	A0A4S2B334	Bacteroidales
	A0A3L8A6H4	Bacteroidales

Figure 13 2'FL supplementation affects faecal bacterial GHs and mucins. Bacterial GHs and (H) their relative protein ID and taxonomy (family). (I–L) Mucins (Muc2, Muc5ac, Muc13, Muc17). One-way ANOVA followed by Tukey post hoc test or Kruskal-Wallis followed by Dunn's test was applied based on data distribution. *p<0.05; **p<0.01; ***p<0.001; ****p<0.0001. 2'FL, 2'-fucosyllactose; ANOVA, analysis of variance; GHs, glycosyl hydrolases; HFD, high-fat diet; ND, not detectable.

While in vitro studies have demonstrated that alterations of the mucus layer may be directly mediated by 2'FL, we cannot exclude the possibility that, in vivo, they are part of a more complex system involving the gut microbiota. As a prebiotic compound, 2'FL can be metabolised by gut bacteria, stimulating, therefore, the proliferation of specific bacterial groups. By analysing the gut microbiota composition, we observed significant clustering according to the diet, with 2'FL supplementation inducing the most significant changes. Specifically, CT and HFD-fed mice were dominated by uncultured *Desulfovibrionaceae*, while

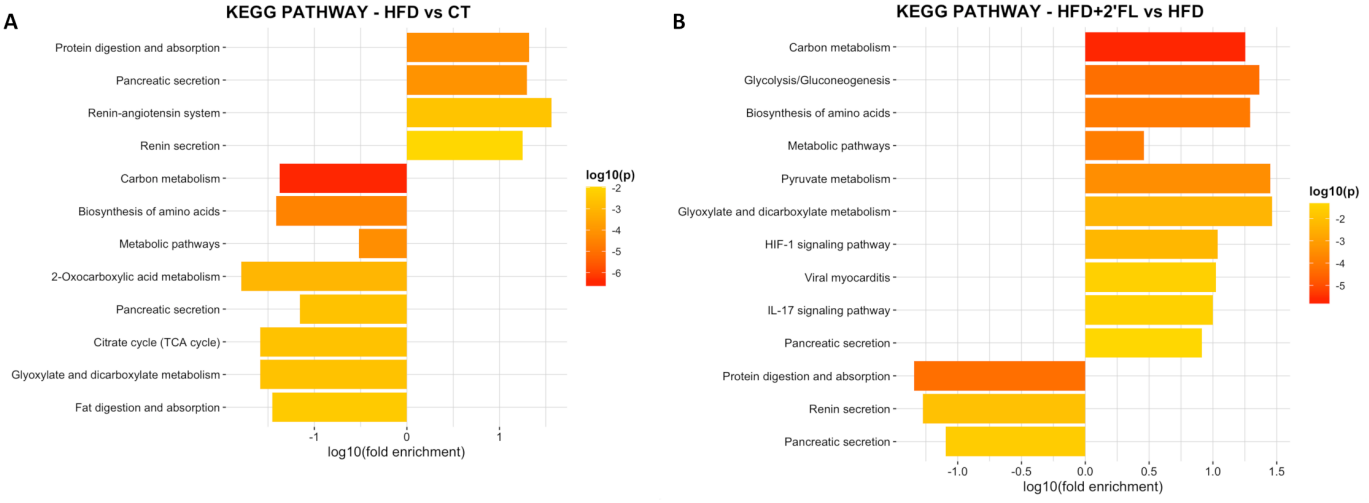

Figure 14 KEGG pathway enrichment analysis performed by using the Database for Annotation, Visualization and Integrated Discovery (DAVID) database. Only significant upregulated and downregulated terms (p<0.05) are shown. 2'FL, 2'-fucosyllactose; HFD, high-fat diet.

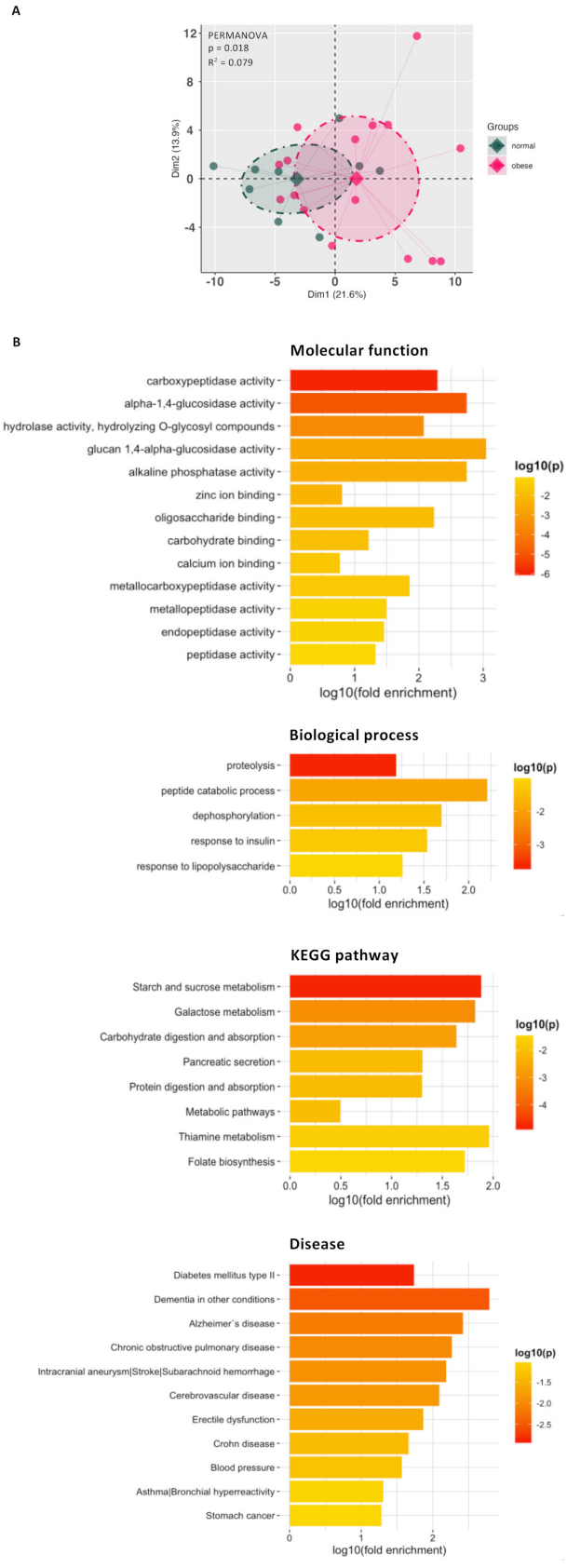

Figure 15 (A) Results of the principal component analysis and permutational multivariate analysis of variance (PERMANOVA) for normal (n=9) and obese (n=16) human subject's proteomes. (B) Enrichment of molecular function, biological process, KEGG pathway and disease in terms of gene ontology (GO) categories. GO categories were determined using DAVID.

Akkermansia and *Bacteroides* were the main bacterial genera in mice receiving 2'FL supplementation. Both genera have been shown to be able to repurpose their mucin degradation machinery for the breakdown of HMOs, reflecting the structural and compositional similarities between HMOs and mucin oligosaccharides.[48 49] It is, therefore, plausible that the effects of 2'FL on metabolism and mucus could be mediated by bacteria that were significantly affected by the treatment. For example, *A. muciniphila*, a species belonging to the genus *Akkermansia*, is a mucin-degrading specialist residing and proliferating in the mucus layer and affecting metabolism in mice and humans.[46 50 51] In mice, *A. muciniphila* was previously reported to counteract HFD-induced obesity and prevent the decrease of mucus layer thickness associated with HFD.[2] On the other hand, *Bacteroides* spp, like *B. uniformis* and *B. acidifaciens*, have been found to be protective against obesity[52–54] and are highly enriched in colonic mucus layer where they can use mucin glycans as energy source.[55] Moreover, WSD-fed rodents display an impaired mucus layer associated with a lower abundance of *Bacteroidetes*[3] and *B. thetaiotaomicron*, increased GC differentiation, increased expression of mucus-related genes and sialylated/sulfated mucins ratio.[56]

Since mice supplemented with 2'FL showed increased mucus production and secretion but no changes in mucus thickness, we next assessed whether 2'FL may have stimulated mucus degradation through enhanced bacterial GH activity. Using in-gel fluorescent ABP labelling, we found increased a-L-fucosidase and a-D-galactosidase activity in 2'FL supplemented mice. The PCA for GHs involved in mucus degradation showed distinct clustering patterns between mice fed HFD+2'FL and those fed CT and HFD diet. Among GHs, two b-D-galactosidases and two a-L-fucosidases, assigned to *Bacteroidales* and *Lachnospiraceae* families, were increased in 2'FL supplemented mice while no differences were observed between CT and HFD groups, where these enzymes were either scarce or absent. Furthermore, we found that 2'FL supplementation significantly increased the levels of b-hexosaminidase and b-*N*-acetylhexosaminidase compared with the CT diet. These results suggest that 2'FL stimulates the production of bacterial GHs involved in mucin glycan degradation, perhaps prompted by their involvement in 2'FL degradation.

Further analysis of the mouse proteome showed that HFD had a profound impact on many proteins participating in metabolic processes. Specifically, HFD upregulated proteins involved in protein digestion and absorption while downregulated those involved in different metabolic pathways, among others. Interestingly, 2'FL supplementation had opposite effects, suggesting its ability to counteract the alteration of metabolic processes induced by the HFD. To gain further insights into the mouse results, we analysed the faecal proteome from obese and lean individuals. We showed that there were significant differences, as previously observed,[57] with some of these changes being similar between HFD-fed mice and obese humans. In addition to obese and lean individuals, even lifestyle-induced weight loss affects proteome.[57 58] In other clinical contexts, faecal proteome has been used to discriminate patients with adenomas and colorectal cancer and novel stool biomarkers have been proposed for early detection, aiming at reducing their incidence and mortality.[59–61] This methodology may be used to define new clinical biomarkers capable of detecting the onset of metabolic disorders, enabling their prevention and monitoring the effectiveness of prebiotic/probiotic treatments or personalised dietary interventions in humans for improving individualised patient care and public health outcomes.

In conclusion, our study demonstrates that 2'FL supplementation in the context of HFD-feeding can counteract obesity and metabolic alterations and it is associated with alterations in the intestinal mucus layer through increased expression of secreted and transmembrane mucins, glycosyltransferases and alterations in mucin glycans composition. These changes were accompanied with different profiles of gut microbiota, faecal proteome and eCB system. Our findings suggest that 2'FL has the potential to improve metabolic outcomes in overweight/obese individuals and highlights the importance of investigating the interaction between mucus and gut microbiota. Together these data pave the way for further research on novel strategies and targets for the prevention and/or treatment of obesity and related disorders.

Author affiliations
[1]Louvain Drug Research Institute (LDRI), Metabolism and Nutrition research group (MNUT), UCLouvain, Université catholique de Louvain, Brussels, Belgium
[2]The Gut Microbiome and Health and Food Safety Institute Strategic Programme, Norwich Research Park, Quadram Institute Bioscience, Norwich, UK
[3]Louvain Drug Research Institute (LDRI), Bioanalysis and Pharmacology of Bioactive Lipids Research Group (BPBL), UCLouvain, Université catholique de Louvain, Brussels, Belgium
[4]de Duve Institute, MASSPROT platform, UCLouvain, Université catholique de Louvain, Brussels, Belgium
[5]Human Microbiome Research Program, Faculty of Medicine, University of Helsinki, Helsinki, Finland
[6]Department Bio-organic Synthesis, Leids Instituut voor Chemisch Onderzoek, Leiden University, Leiden, The Netherlands
[7]Department of Medical Biochemistry and Cell Biology, Institute of Biomedicine, University of Gothenburg, Gothenburg, Sweden
[8]Walloon Excellence in Life Sciences and BIOtechnology (WELBIO) Department, WEL Research Institute, Wavre, Belgium
[9]Institute of Experimental and Clinical Research (IREC), IREC Imaging Platform (2IP RRID:SCR_023378), UCLouvain, Université catholique de Louvain, Brussels, Belgium
[10]Institute of Experimental and Clinical Research (IREC), UCLouvain, Université catholique de Louvain, Brussels, Belgium

X Paola Paone @Paola_9229, Nathalie Juge @JugeLab and Matthias Van Hul @matthias_vanhul

Acknowledgements We thank H. Danthinne, B. Es Saadi, L. Gesche and R. M. Goebbels (at UCLouvain, Université catholique de Louvain) for their excellent technical support and assistance. We thank A. Daumerie from the IREC imagery platform (2IP) from the Institut de Recherche Expérimentale et Clinique (IREC) for the excellent help. We thank NK Nguyen for performing PCA in figure 15A. Figure 7 was created using BioRender.com. F. Suriano is currently employee at European Food Safety Authority, Via Carlo Magno 1A, 43126, Parma, Italy.

Contributors PP and PDC conceived and designed the study. PP performed the experiments and data analysis. AP performed analysis. PP and PDC performed the interpretation. PP prepared the samples for sequencing. PP and CJ processed the sequences and performed the bioinformatics and statistical analysis for the gut microbiota. DL and NJ performed the mucin glycans composition analysis and PP and PDC interpreted the results. RT and GGM performed the analysis of lipids and endocannabinoids. MEVJ and FS helped for the mucus protocol. CB, MVH and AP helped for all the histological analysis. VB helped for ABP-labelling. BIF contributed for proteomic, Nano-LC-MS settings for pulldown samples and MaxQuant processing. DV contributed for processing MS/MS data from MASCOT Generic Format files from human faecal proteomes. PP performed proteomic analysis and interpretation in Perseus, MetaboAnalysist and DAVID. PDC and HO contributed to financial resources. PDC and MVH supervised the lab work. PP and PDC wrote the first version of the paper. All authors critically revised the manuscript and approved the final version before submission. PDC is the guarantor of this study.

Funding European Union's Horizon 2020 research and innovation program (H2020 Marie Skłodowska-Curie Actions under the agreement no: 814102 ITN H2020 MSCA Sweet Crosstalk). PDC is honorary research director at Fonds de la Recherche Scientifique (FNRS) and is recipients of grants from FNRS (Projet de Recherche PDR-convention: FNRS T.0030.21, CDR-convention: J.0027.22, FRFS-WELBIO: WELBIO-CR-2019C-02R, WELBIO-CR-2022A-02, EOS: program no. 40007505). Fédération Wallonie-BruxellesARC19/24-096. La Caixa foundation (NeuroGut).

Competing interests PDC is an editor of the journal. PDC is inventor on patent applications dealing with the use bacteria on metabolic disorders. PDC was cofounders of The Akkermansia company SA and Enterosys.

Patient and public involvement Patients and/or the public were not involved in the design, or conduct, or reporting, or dissemination plans of this research.

Patient consent for publication Consent obtained directly from patient(s).

Ethics approval The mouse experiments were approved by and performed following the guidelines of the local ethics committee for animal care of the Health Sector of the Université catholique de Louvain under the specific agreement number 2017/UCL/MD/005. Animal housing conditions were as specified by the Belgian Law of 29 May 2013 regarding the protection of laboratory animals (Agreement number LA 1230314). This study involves human participants and human faecal samples were obtained from a previous study (Kolmeder et al, ref 57) and this observational study was approved by the Medical Ethics Committee of the Atrium Medical Center (Heerlen, the Netherlands; registration number NL30502.096.09). Participants gave informed consent to participate in the study before taking part.

Provenance and peer review Not commissioned; externally peer reviewed.

Data availability statement All data relevant to the study are included in the article or uploaded as online supplemental information. All data generated or analysed during this study are included in this published article and its online supplemental information files. The raw amplicon sequencing data analysed in this study have been deposited in the European Nucleotide Archive (ENA) at EMBL-EBI under accession number PRJEB72192. The mass spectrometry proteomics data have been deposited to the ProteomeXchange Consortium via the PRIDE [62] partner repository with the dataset identifier PXD049406.

ORCID iDs
Paola Paone http://orcid.org/0009-0000-9385-9890
Dimitris Latousakis http://orcid.org/0000-0002-2472-9328
Didier Vertommen http://orcid.org/0000-0001-7648-8282
Ching Jian http://orcid.org/0000-0003-0577-8834
Valentina Borlandelli http://orcid.org/0000-0002-5003-8678
Francesco Suriano http://orcid.org/0000-0002-1343-5500
Malin E V Johansson http://orcid.org/0000-0002-4237-6677
Caroline Bouzin http://orcid.org/0000-0003-0694-1947
Nathalie M Delzenne http://orcid.org/0000-0003-2115-6082
Anne Salonen http://orcid.org/0000-0002-6960-7447
Nathalie Juge http://orcid.org/0000-0001-8515-1315
Bogdan I Florea http://orcid.org/0000-0001-7114-2266
Giulio G Muccioli http://orcid.org/0000-0002-1600-9259
Herman Overkleeft http://orcid.org/0000-0001-6976-7005
Matthias Van Hul http://orcid.org/0000-0002-5503-107X
Patrice D Cani http://orcid.org/0000-0003-2040-2448

REFERENCES

1 Cani PD. Human gut microbiome: hopes, threats and promises. *Gut* 2018;67:1716–25.
2 Everard A, Belzer C, Geurts L, *et al*. Cross-talk between Akkermansia Muciniphila and intestinal epithelium controls diet-induced obesity. *Proc Natl Acad Sci U S A* 2013;110:9066–71.
3 Schroeder BO, Birchenough GMH, Ståhlman M, *et al*. Bifidobacteria or fiber protects against diet-induced microbiota-mediated colonic mucus deterioration. *Cell Host Microbe* 2018;23:27–40.
4 Schroeder BO, Birchenough GMH, Pradhan M, *et al*. Obesity-associated microbiota contributes to mucus layer defects in genetically obese mice. *J Biol Chem* 2020;295:15712–26.
5 Mastrodonato M, Mentino D, Portincasa P, *et al*. High-fat diet alters the oligosaccharide chains of colon Mucins in mice. *Histochem Cell Biol* 2014;142:449–59.
6 Desai MS, Seekatz AM, Koropatkin NM, *et al*. A dietary fiber-deprived gut microbiota degrades the Colonic mucus barrier and enhances pathogen susceptibility. *Cell* 2016;167:1339–53.

7 Mastrodonato M, Calamita G, Mentino D, *et al*. High-fat diet alters the glycosylation patterns of duodenal mucins in a murine model. *J Histochem Cytochem* 2020;68:279–94.
8 Birchenough GMH, Schroeder BO, Sharba S, *et al*. Muc2-dependent microbial colonization of the jejunal mucus layer is diet sensitive and confers local resistance to enteric pathogen infection. *Cell Rep* 2023;42:112084.
9 Chassaing B, Raja SM, Lewis JD, *et al*. Colonic microbiota encroachment correlates with dysglycemia in humans. *Cell Mol Gastroenterol Hepatol* 2017;4:205–21.
10 Paone P, Cani PD. Mucus barrier, mucins and gut microbiota: the expected slimy partners? *Gut* 2020;69:2232–43.
11 Hu M, Zhang X, Li J, *et al*. Fucosyltransferase 2: a genetic risk factor for intestinal diseases. *Front Microbiol* 2022;13:940196.
12 Rausch P, Rehman A, Künzel S, *et al*. Colonic mucosa-associated microbiota is influenced by an interaction of Crohn disease and FUT2 (Secretor) genotype. *Proc Natl Acad Sci U S A* 2011;108:19030–5.
13 Imhann F, Vich Vila A, Bonder MJ, *et al*. Interplay of host genetics and gut microbiota underlying the onset and clinical presentation of inflammatory bowel disease. *Gut* 2018;67:108–19.
14 Tong M, McHardy I, Ruegger P, *et al*. Reprograming of gut microbiome energy metabolism by the FUT2 Crohn's disease risk polymorphism. *ISME J* 2014;8:2193–206.
15 Wacklin P, Tuimala J, Nikkilä J, *et al*. Faecal microbiota composition in adults is associated with the FUT2 gene determining the secretor status. *PLoS One* 2014;9:e94863.
16 Castanys-Muñoz E, Martin MJ, Prieto PA. 2′-Fucosyllactose: an abundant, genetically determined soluble Glycan present in human milk. *Nutr Rev* 2013;71:773–89.
17 Lewis ZT, Totten SM, Smilowitz JT, *et al*. Maternal fucosyltransferase 2 status affects the gut bifidobacterial communities of breastfed infants. *Microbiome* 2015;3:13.
18 Zhu Y, Wan L, Li W, *et al*. Recent advances on 2′-Fucosyllactose: physiological properties, applications, and production approaches. *Crit Rev Food Sci Nutr* 2022;62:2083–92.
19 Sanz Morales P, Wijeyesekera A, Robertson MD, *et al*. The potential role of human milk oligosaccharides in irritable bowel syndrome. *Microorganisms* 2022;10:2338.
20 Lee S, Goodson M, Vang W, *et al*. 2′-Fucosyllactose supplementation improves gut-brain signaling and diet-induced obese phenotype and changes the gut microbiota in high Fat-Fed mice. *Nutrients* 2020;12:1003.
21 Lee S, Goodson ML, Vang W, *et al*. Human milk oligosaccharide 2′-Fucosyllactose supplementation improves gut barrier function and signaling in the vagal afferent pathway in mice. *Food Funct* 2021;12:8507–21.
22 Wu RY, Li B, Koike Y, *et al*. Human milk oligosaccharides increase mucin expression in experimental necrotizing enterocolitis. *Mol Nutr Food Res* 2019;63:e1800658.
23 Cheng L, Kong C, Walvoort MTC, *et al*. Human milk oligosaccharides differently modulate goblet cells under homeostatic, proinflammatory conditions and ER stress. *Mol Nutr Food Res* 2020;64:1900976.
24 Muccioli GG, Naslain D, Bäckhed F, *et al*. The endocannabinoid system links gut microbiota to adipogenesis. *Mol Syst Biol* 2010;6:392.
25 Manca C, Boubertakh B, Leblanc N, *et al*. Germ-free mice exhibit profound gut microbiota-dependent alterations of intestinal endocannabinoidome signaling. *J Lipid Res* 2020;61:70–85.
26 Shen M, Manca C, Suriano F, *et al*. Three of a kind: control of the expression of liver-expressed antimicrobial peptide 2 (LEAP2) by the endocannabinoidome and the gut microbiome. *Molecules* 2021;27:1.
27 Suriano F, Manca C, Flamand N, *et al*. A lipidomics- and transcriptomics-based analysis of the intestine of genetically obese (OB/OB) and diabetic (dB/dB) mice: links with inflammation and gut microbiota. *Cells* 2023;12:411.
28 Jiang J, Kallemeijn WW, Wright DW, *et al*. In vitro and in vivo comparative and competitive activity-based protein profiling of GH29 α-L-fucosidases. *Chem Sci* 2015;6:2782–9.
29 Willems LI, Beenakker TJM, Murray B, *et al*. Potent and selective activity-based probes for GH27 human retaining α-Galactosidases. *J Am Chem Soc* 2014;136:11622–5.
30 Yao Q, Li H, Gao Y, *et al*. The milk active ingredient, 2′-Fucosyllactose, inhibits inflammation and promotes MUC2 secretion in LS174T goblet cells in vitro. *Foods* 2023;12:186.
31 Wu RY, Botts SR, Johnson-Henry KC, *et al*. Variations in the composition of human milk oligosaccharides correlates with effects on both the intestinal epithelial barrier and host inflammation: a pilot study. *Nutrients* 2022;14:1014.
32 Kong C, Elderman M, Cheng L, *et al*. Modulation of intestinal epithelial glycocalyx development by human milk oligosaccharides and non-digestible carbohydrates. *Mol Nutr Food Res* 2019;63:1900303.
33 Qu D, Wang G, Yu L, *et al*. The effects of diet and gut microbiota on the regulation of intestinal Mucin Glycosylation. *Carbohydr Polym* 2021;258:117651.
34 Paone P, Suriano F, Jian C, *et al*. Prebiotic oligofructose protects against high-fat diet-induced obesity by changing the gut microbiota, intestinal mucus production, glycosylation and secretion. *Gut Microbes* 2022;14:2152307.
35 Maroni L, Hohenester SD, van de Graaf SFJ, *et al*. Knockout of the primary sclerosing cholangitis-risk gene Fut2 causes liver disease in mice. *Hepatology* 2017;66:542–54.
36 Zhou R, Llorente C, Cao J, *et al*. Intestinal **A**1-2-Fucosylation contributes to obesity and steatohepatitis in mice. *Cell Mol Gastroenterol Hepatol* 2021;12:293–320.
37 Larsson JMH, Karlsson H, Sjövall H, *et al*. A complex, but uniform O-Glycosylation of the human MUC2 mucin from colonic biopsies analyzed by nanoLC/Msn. *Glycobiology* 2009;19:756–66.
38 Larsson JMH, Karlsson H, Crespo JG, *et al*. Altered O-Glycosylation profile of Muc2 Mucin occurs in active ulcerative colitis and is associated with increased inflammation. *Inflamm Bowel Dis* 2011;17:2299–307.
39 Itzkowitz SH, Yuan M, Montgomery CK, *et al*. Expression of Tn, Sialosyl-Tn, and T antigens in human colon cancer. *Cancer Res* 1989;49:197–204.
40 Orntoft TF, Harving N, Langkilde NC. O-linked Mucin-type glycoproteins in normal and malignant colon mucosa: lack of T-antigen expression and accumulation of Tn and Sialosyl-Tn antigens in carcinomas. *Int J Cancer* 1990;45:666–72.
41 Juge N. Relationship between mucosa-associated gut Microbiota and human diseases. *Biochem Soc Trans* 2022;50:1225–36.
42 Bergstrom K, Shan X, Casero D, *et al*. Proximal colon-derived O-glycosylated mucus encapsulates and modulates the microbiota. *Science* 2020;370:467–72.
43 de Vos WM, Tilg H, Van Hul M, *et al*. Gut microbiome and health: mechanistic insights. *Gut* 2022;71:1020–32.
44 Suzuki H, Bouhnik J, Alhenc-Gelas F, *et al*. Direct radioimmunoassay for rat high molecular weight Kininogen. measurement of immunoreactive high molecular weight Kininogen in normal and Kininogen deficient plasma. *Agents Actions Suppl* 1987;22:277–87.
45 Depommier C, Vitale RM, Iannotti FA, *et al*. Beneficial effects of Akkermansia Muciniphila are not associated with major changes in the circulating Endocannabinoidome but linked to higher mono-Palmitoyl-glycerol levels as new PPARα agonists. *Cells* 2021;10:185.
46 Depommier C, Everard A, Druart C, *et al*. Supplementation with Akkermansia Muciniphila in overweight and obese human volunteers: a proof-of-concept exploratory study. *Nat Med* 2019;25:1096–103.
47 Hansen KB, Rosenkilde MM, Knop FK, *et al*. 2-Oleoyl glycerol is a GPR119 agonist and signals GLP-1 release in humans. *J Clin Endocrinol Metab* 2011;96:E1409–17.
48 Marcobal A, Sonnenburg JL. Human milk oligosaccharide consumption by intestinal microbiota. *Clin Microbiol Infect* 2012;18 Suppl 4:12–5.
49 Salli K, Hirvonen J, Siitonen J, *et al*. Selective utilization of the human milk oligosaccharides 2′-Fucosyllactose, 3-fucosyllactose, and difucosyllactose by various probiotic and pathogenic bacteria. *J Agric Food Chem* 2021;69:170–82.
50 Belzer C, de Vos WM. Microbes inside--from diversity to function: the case of Akkermansia. *ISME J* 2012;6:1449–58.
51 Cani PD, de Vos WM. Next-generation beneficial microbes: the case of Akkermansia Muciniphila *Front Microbiol* 2017;8:1765.
52 Yoshida N, Yamashita T, Osone T, *et al*. Bacteroides Spp. promotes branched-chain amino acid catabolism in Brown fat and inhibits obesity. *iScience* 2021;24:103342.
53 Gauffin Cano P, Santacruz A, Moya Á, *et al*. Bacteroides Uniformis CECT 7771 ameliorates metabolic and immunological dysfunction in mice with high-fat-diet induced obesity. *PLoS One* 2012;7:e41079.
54 Yang J-Y, Lee Y-S, Kim Y, *et al*. Gut commensal bacteroides acidifaciens prevents obesity and improves insulin sensitivity in mice. *Mucosal Immunol* 2017;10:104–16.
55 Tan H, Zhai Q, Chen W. Investigations of Bacteroides Spp. towards next-generation probiotics. *Food Res Int* 2019;116:637–44.
56 Wrzosek L, Miquel S, Noordine M-L, *et al*. Bacteroides Thetaiotaomicron and Faecalibacterium Prausnitzii influence the production of mucus glycans and the development of goblet cells in the colonic epithelium of a gnotobiotic model rodent. *BMC Biol* 2013;11:61.
57 Kolmeder CA, Ritari J, Verdam FJ, *et al*. Colonic metaproteomic signatures of active bacteria and the host in obesity. *Proteomics* 2015;15:3544–52.
58 Biemann R, Buß E, Benndorf D, *et al*. Fecal metaproteomics reveals reduced gut inflammation and changed microbial metabolism following lifestyle-induced weight loss. *Biomolecules* 2021;11:726.
59 Bosch S, Acharjee A, Quraishi MN, *et al*. Integration of stool microbiota, proteome and amino acid profiles to discriminate patients with adenomas and colorectal cancer. *Gut Microbes* 2022;14:2139979.
60 Long S, Yang Y, Shen C, *et al*. Metaproteomics characterizes human gut microbiome function in colorectal cancer. *NPJ Biofilms Microbiomes* 2020;6:14.
61 Komor MA, Bosch LJ, Coupé VM, *et al*. Proteins in stool as biomarkers for non-invasive detection of colorectal adenomas with high risk of progression. *J Pathol* 2020;250:288–98.
62 Perez-Riverol Y, Bai J, Bandla C, *et al*. The PRIDE database resources in 2022: a hub for mass spectrometry-based proteomics evidences. *Nucleic Acids Res* 2022;50:D543–52.

MATERIALS AND METHODS

Mice and diets

Seven-week-old male C57BL/6J mice (Janvier, Le Genest-Saint-Isle, France) were co-housed in pairs under Specific and Opportunistic Pathogen Free conditions (SOPF) in a controlled environment (temperature of 22 ± 2 °C, 12-h daylight cycle) with free access to food and water. Upon arrival, all the mice underwent a 1-week acclimatization period, during which they were fed a control diet [1] (AIN93Mi, Research Diet, New Brunswick, NJ, USA).

A set of 30 mice was randomly divided into 3 groups of 12 mice: 1) CT group, fed a control diet 2) HFD group, fed a high-fat diet (60% fat and 20% carbohydrates (kcal/100g), D12492, Research diet, New Brunswick, NJ, USA), and 3) HFD+2'FL group, fed a HFD diet supplemented with 10% of prebiotic 2'-fucosyllactose added in drinking water (DSM, Denmark). The dose of 10% of 2'FL represents the effective dose to elicit metabolic effects.[2,3] The treatment continued for 6 weeks.

Body weight, food and water intake were recorded three times per week. Body composition was assessed once a week by using a 7.5-MHz time-domain nuclear magnetic resonance (LF50 minispec; Bruker, Rheinstetten, Germany). Feces were harvested weekly since the beginning (Day 0), until the end of the experiment (Day 45). All mouse experiments were approved by and performed in accordance with the guidelines of the local ethics committee. Housing conditions were specified by the Belgian Law of 29 May 2013, regarding the protection of laboratory animals (agreement number LA1230314).

Oral Glucose Tolerance Test

One week before the end of experiment, the mice were fasted for 6 hours before receiving an oral gavage glucose load (2 g glucose per kg body weight). Blood glucose was measured 30 minutes before (time point -30), just prior the oral glucose load (time point 0) and then after 15, 30, 60, 90 and 120 minutes. Blood glucose was determined with a glucose meter (Accu Check, Roche, Switzerland) on blood samples collected from the tip of the tail vein.

Tissue sampling

At the end of the experiment (week 6) and after 6h of fasting, all mice were anesthetized with isoflurane (Forene®, Abbott, Queenborough, Kent, England) and blood was collected from the

portal and cava veins. Then, the mice were immediately euthanized by cervical dislocation. Adipose depots (epididymal, subcutaneous, visceral and brown), muscles (tibialis anterior, vastus lateralis, gastrocnemius, soleus) and intestinal segments (jejunum, ileum, caecum and colon) were dissected, weighed and immersed in liquid nitrogen before long-term storage at −80 °C for further analysis.

One segment of colon from each mouse was opened, without flushing it before, for the collection of the mucus layer by gently scraping with a microscope glass slide and then weighed.

Biochemical Analysis

To determine the plasma insulin concentration, blood was harvested from the tip of the tail vein using capillaries prior to glucose load (−30 min) and 15 min after glucose load. Plasma insulin concentration was measured using an ELISA kit (Mercodia, Uppsala, Sweden), according to the manufacturer's instructions. Insulin resistance index was determined by multiplying the area under the curve of the blood glucose (−30 to 15 min) and plasma insulin (-30 min and 15 min).

Plasma Multiplex Analysis

Plasma levels of glucagon-like peptide 1 (GLP-1), peptide YY (PYY), ghrelin, leptin and glucagon were measured from the portal vein by multiplex assay kits based on chemiluminescence detection and following manufacturer's instructions (Meso Scale Discovery (MSD), Gaithersburg, MD, USA). Analyses were performed using a QuickPlex SQ 120 instrument (MSD) and DISCOVERY WORKBENCH® 4.0 software (MSD, Rockville, MD, USA).

RNA Preparation and gene expression analysis by real-time qPCR analysis

Total RNA was prepared from tissues using TriPure reagent (Roche). Quantification and integrity analysis of total RNA was performed by running 1 µl of each sample on an Agilent 2100 Bioanalyzer (Agilent RNA 6000 Nano Kit, Agilent). cDNA was prepared by reverse transcription of 1 µg total RNA using a Reverse Transcription System kit (Promega, Leiden, The Netherlands). Real-time PCRs were performed with the StepOnePlus real-time PCR system and software (Applied Biosystems, Den Ijssel, The Netherlands) using Mesa Fast qPCR sybr green mix (Eurogentec, Seraing, Belgium) and with the CFX Manager 3.1 software (Bio-

Rad, Hercules, CA) using Mesa Fast qPCR (GoTaq qPCR Master Mix, Promega, Madison, WI, USA) for detection, according to the manufacturer's instructions. RPL19 was chosen as housekeeping gene. All samples were run in duplicate in a single 96-well reaction plate, and data were analyzed according to the 2- ΔΔCt method. The identity and purity of the amplified product was checked through analysis of the melting curve carried out at the end of amplification. Primer sequences for the targeted mouse genes are available in Supplemental Table 9.

Analysis of the mucus layer thickness, goblet cells and immunohistochemistry

Colon segments were immediately removed and fixed in Carnoy's solution (ethanol 6: acid acetic 3: chloroform 1, vol/vol) for 2h at 4 °C. They were then immersed in ethanol 100% for 24 h. For the analysis of the mucus layer thickness and goblet cells, paraffin sections of 5 µm were stained with alcian blue. Images were captured at × 20 magnification and obtained using a SNC400 slide scanner and digital Image Hub software 561 (Leica Biosystems, Wetzlar, Germany). Analyses were performed using ImageJ (version 1.48r, National Institutes of Health, Bethesda, Maryland, USA) in a blinded manner. For the mucus layer thickness, two to six fields were used for each mouse and a minimum of 20 different measurements were made perpendicular to the inner mucus layer per field. For the goblet cells, the luminal side, muscularis mucosae, submucosa and muscle layer were removed and the blue area and the total area were measured separately in the remaining mucosal part of the colon. The proportion of the goblet cells was quantified based on the ratio between the blue area over the total area.

Histology and Fluorescent in situ hybridization

Segments of the distal colon from mice were fixed in water-free Methanol-Carnoy's fixative [60% methanol, 10% chloroform and 30% acetic acid] before paraffin embedding. Paraffin sections were dewaxed with Xylene substitute and hybridized with a general bacterial probe, EUB 338 conjugated to C3 (Merck, Ref: MBD0033). Immunostaining after hybridizations was performed with anti-MUC2C3 antiserum as described previously [4]. Pictures were obtained with a LSM800 confocal microscope from Zeiss.

Bacterial distance and density

The bacterial penetration of the mucus was assessed using two parameters: the distance from the bacterial front to the epithelial cells and the density of bacterial cells within the inner mucus layer. The location of the bacterial front was easily delineated as the outermost border of the zone with high intensity for bacterial stain. The inner mucus was defined as the MUC2 positive layer between the bacterial front and the epithelial cells. To assess the first parameter, at least 10 pictures from different locations of at least 2 different distant sections were analyzed per mouse, with at least 10 measurements (distance between bacterial front and closest epithelial cell) taken per pictures to determine the average distance between the bacterial front and the apical side of the epithelial cells. For the second parameter, the bacterial density of the inner mucus, the area of the MUC2 positive layer between the bacterial front and the epithelial cells was measured and bacteria within this layer were counted manually by two independent investigators in a blinded manner. For this analysis, at least 5 pictures were analyzed per mouse. Analyses were performed using (Fiji Is Just) ImageJ 2.14.0/1.54f For Mac OS and 2.14.0 for Windows. Measurements were first averaged per section, then per mouse, then per group.

Mucin glycan extraction and composition

Colonic mucus was suspended in 400 µl mucin extraction buffer (0.2 M Tris, pH 8, 1% SDS, 10 mM DTT). The samples were incubated at 60°C for 90 min. Iodoacetamide was added from a 1M stock solution to a final concentration of 100 mM. The samples were incubated at RT for 90 min in dark. The reduced samples were spin filtered through a 100k MWCO amicon 0.5 filter (merck) for 15 min at 14000 g. Lithium dodecyl sulphate (LDS) loading buffer (10 µl; Thermo Fischer) was added to the samples and loaded onto a 1% vertical agarose gel cast in Tris-Glycine-SDS (TGS) buffer (Biorad). Vertical agarose gel electrophoresis (VAGE) was carried out at 100 V for 45 min. The mucins/proteins were transferred onto Immobilon Psq(Merck) in Tris-glycine [5] buffer, using Trans-blot Turbo (25 V, 1 A, 60 min; Biorad). The region of the blot were mucins migrated was cut out and the blot was immersed into 500 µl 0.5M $NaBH_4$ in 0.05 M NaOH. The β-elimination reactions were incubated at 45°C for 16 h and quenched by the stepwise addition of 1ml 5% aqueous acetic acid. The samples were desalted on in-house prepared cation exchange columns using Amberlite 50Wx8 H+ 200-400mesh. The

samples were dried under vacuum and removal of borates was carried out with co-evaporation with methanol under nitrogen.

For the base required for permethylation, 400 µl of 50% NaOH were mixed with 800 µl dry MeOH and 4 ml of anhydrous DMSO. The resulting gel was washed 5 times with 4 ml DMSO before resuspended in 4 ml DMSO. The dried samples were dissolved in 100 µl anhydrous DMSO, followed by the addition of 150 µl of the prepared base and 75µl of iodomethane. The samples were vortexed for 2 h at 2000 rpm and the reactions were quenched by the addition of 500 µl H2O. Excess of iodomethane was removed with a flow of nitrogen.

The permethylated glycans were loaded onto a Swift-HLB cartridge (Merck). Salts and other hydrophilic contaminants were removed with 4x1 ml washes with H2O and permethylated glycans were eluted with 4x1 ml of MeOH. The eluted glycans were dried under vacuum and redissolved in 10 µl of 30% acetonitrile in 0.1% aqueous trifluoroacetic acid (TA30). The sample (0.5 µl) was mixed with 0.5 µl of 2,5-dehydroxy-benzoic acid (DHB, 20 mg/ml in TA30) and spotted onto a MTP ground steel MALDI target plate. The samples were analysed by MALDI-ToF MS on a Bruker Autoflex in positive reflectron mode. Peak detection and integration in the mass spectra was done using flexAnalysis (v3.4, Bruker Daltonics) with the following settings: Peak detection algorithm was Snap2, signal to noise threshold = 2, relative intensity threshold = 0, minimum intensity threshold = 2, SNAP2 average composition was set to “sugar”, baseline subtraction was set to TopHat. Relative abundance of each peak identified as glycan was calculated as the area of the peak over the sum of all peaks that were identified as glycans. Only glycans present in at least 3 mice and in at least one group were shown.

Endocannabinoid and lipid content

The endocannabinoid and lipid content in the cecal tissue was analyzed by UHPLC-MS. Briefly, lipids were extracted by ultraturax homogeneisation and internal standards (d_4-AEA, d_4-PEA, d_4-OEA, d_4-SEA and d_5-1-2-AG) were added, followed by protein precipitation (acetone) and recover the supernatant. The samples were analyzed with Xevo-TQS mass spectrometer (from Waters). Absolute quantifications were obtained first by normalizing the area under the curve [6] of the lipid species with the AUC of the respective internal standard and second by extrapolation of the compound’s ratio in his own calibration curve. The LC-MS methods was the following: BEH LC-18 column 50*2.1, 1.7µm (Waters) at 40°C. The mobile phase consisted

in a gradient between A: H_2O 25% -MeOH 75%; B: MeOH 100%, all containing acetic acid (0.1%). ESI probe operated in positive mode was also used for sample ionization. The mass spectrometer parameters were the following: capillary voltage: 2.9kV ; cone voltage : 30V ; desolvation temperature : 550°C ; desolvation gas flow : 1100L/Hr : cone gas flow : 170L/Hr : nebuliser : 6bar.

DNA extraction and 16S rRNA gene amplicon sequencing

Analysis of gut microbiota composition was performed for fecal samples collected at the beginning (day 0) and at the end (day 45) of the study and for the caecal content collected and kept frozen at -80°C until use. Genomic DNA was extracted using a QIAamp DNA Stool Mini Kit (Qiagen, Hilden, Germany), according to the manufacturer's instructions, including a bead-beating step. The V4 region of the bacterial 16S rRNA gene was amplified with the primers 515F(GTGYCAGCMGCCGCGGTAA) and 806R (GGACTACNVGGGTWTCTAAT). Purified amplicons were sequenced using Illumina MiSeq technology following the manufacturer's guidelines. Sequencing was performed at MR DNA (www.mrdnalab.com; Shallowater, TX). Sequences were processed using the QIIME2 pipeline (version 2021.4).[7] Demultiplexed 225-bp paired-end sequences were denoised using DADA2 to obtain an amplicon sequence variant (ASV) table.[8] Singletons (ASV present < 2 times) and ASVs present in less than 10% of the samples were discarded. Taxonomic classification was performed using a pre-trained naive Bayes classifier implemented in QIIME2 against the SILVA 132 reference database.[9] Taxa that could not be identified on genus-level are referred to the highest taxonomic rank identified.

Quantitative PCR for total bacteria

Quantification of total bacteria was carried out by qPCR with universal bacterial primers (338F: ACTCCTACGGGAGGCAGCAG, 518R: ATTACCGCGGCTGCTGG), with the StepOnePlus real-time PCR system and software (Applied Biosystems, Den Ijssel, The Netherlands) using GoTaq qPCR sybr green mix (Promega, Madison, Wisconsin, USA), according to the manufacturer's instructions. All samples were run in duplicate in a single 96-well reaction plate. The cycle threshold [1] of each sample was compared with a standard curve made by serially diluting genomic DNA isolated from a pure culture of the type strain of *Lactobacillus acidophilus* (DSM 20079 01-21) (BCCM/LMG, Ghent, Belgium; DSMZ, Braunshweig, Germany).

The absolute abundances of individual bacterial genera were estimated by multiplying their relative abundance by total bacterial density as described previously.[10]

Preparation of mouse fecal extracts

Fecal extracts were processed based on the protocol of Redinbo et al.[11], with modifications. Briefly, 1-2 fecal pellets collected at the end of the experiment and stores at -80 °C were rehydrated with 350 µl cold extraction buffer (pH 6.5, 25 mM HEPES, 25 mM NaCl with Roche cOmpleteTM protease inhibitor cocktail). The mixture was then transferred in new tubes containing autoclaved 0.7 mm garnet beads and vortexed to break up dense and fibrous material. Bacterial cells were lysed using MP FastPrep-24^{TM} Classic high-speed benchtop homogenizer (MP Biomedicals, Santa Ana, CA, USA) for 2 minutes at 30 Hertz. The resulting homogenate was sonicated two times for 2 min, with an intermediate step of mixing by inversion. The resulting homogenate was centrifugated at 13,000xg for 10 min at 4 °C and the supernatant was decanted. The total protein concentration was calculated using Pierce^{TM} BCA Protein Assay Kit (#23225, Thermo Fisher Scientific, Waltham, MA, USA). The mouse fecal extract was aliquoted and stored at -80°C until further use.

In-gel activity-based probes (ABP) fluorescent labelling of mouse fecal extracts

Mouse fecal extracts were diluted with buffer (pH 6.5, 125 mM HEPES, 125 mM NaCl, final) to have 1 µg of total protein in 9 µL of lysate working solution. 1 µL of Cy5-ABP at a final concentration of 1 µM for alpha-L-fucosidase labeling (JJB381)[12] and 0.5 µM for alpha-D-galactosidase (TB474)[13] was added to the lysate working solution (9 µL) on ice, and the resulting mixture was incubated at 37 °C for 1 h. The samples were denatured by adding 2.5 µL 5x Laemmli buffer (containing 0.3 M Tris-HCl pH 6.8, 50 % (v/v) 100 % glycerol, 8 % (w/v) dithiothreitol (DTT), 10 % (w/v) sodium dodecyl sulfate (SDS), 0.01 % (w/v) bromophenol blue) and boiled at 98 °C for 5 min. Samples were cooled on ice and run on 1.00 mm 10% polyacrylamide gel at 200 V. Wet-slab gels were scanned for ABP-emitted fluorescence using the Typhoon^{TM} FLA 9500 scanner (Amersham Biosciences, Piscataway, NJ, USA), at 700 PMT and 50 µm resolution. Wet-slab gels were subsequently stained with Coomassie Brilliant Blue (CBB) staining agent to verify accurate protein loading. Full gel images and the relative CBB scanned images can be found in Supplemental Figure 7A,B.

Total proteomic analysis of mouse fecal extracts

5 µg of proteins from mouse fecal extracts were diluted in 5 µL of buffer (pH 6.5, 125 mM HEPES, 125 mM NaCl, final). 100 µL 8 M urea/100 mM ammonium bicarbonate (pH 8) were added to each sample and shacked for 30 minutes, 25 °C, 800 rpm to denature the proteins. Samples were reduced with 10 µL of 20 mM DTT and incubated for 30 minutes at 37 °C and shacked at 800 rpm. The samples were cooled at RT for 10 minutes and then 10 µL 50 mM iodoacetamide (IAA) were added. The samples were incubated in the dark at RT for 30 minutes. 900 µL 20 mM ammonium bicarbonate (pH 8) were added to each sample and then 200 ng of trypsin were added to digest the proteins. The samples were incubated overnight at 37°C and shacked at 500 rpm. The following day, to lower the pH to pH < 3, 10 µL of formic acid (FA) were added. The samples were desalted using stage tips and prepared for LC/MS analysis.

Nano-LC-MS settings for total proteomic analysis

Desalted peptide samples were reconstituted in 30 µL LC-MS solution (97:3:0.1 H_2O, CH_3CN, FA) containing 10 fmol/µL yeast enolase digest (cat. 186002325, Waters) as injection control. Injection amount was titrated using a pooled quality control sample to prevent overloading the nanoLC system and the automatic gain control (AGC) of the QExactive mass spectrometer. The desalted peptides were separated on an UltiMate 3000 RSLCnano system set in a trap-elute configuration with a nanoEase M/Z Symmetry C18 100 Å, 5 µm, 180 µm x 20 mm (Waters) trap column for peptide loading/retention and nanoEase M/Z HSS C18 T3 100 Å, 1.8 µm, 75 µm x 250 mm (Waters) analytical column for peptide separation. The column was kept at 40 °C in a column oven. Samples were injected on the trap column at a flow rate of 15 µL/min for 2 min with 99% mobile phase A (0.1% FA in ULC-MS grade water (Biosolve)), 1% mobile phase B (0.1% FA in ULC-MS grade acetonitrile (Biosolve)) eluent. The 85 min LC method, using mobile phase A and mobile phase B controlled by a flow sensor at 0.3 µL/min with average pressure of 400-500 bar (5500-7000 psi), was programmed as gradient with linear increment to 1% B from 0 to 2 min, 5% B at 5 min, 22% B at 55 min, 40% B at 64 min, 90% B at 65 to 74 min and 1% B at 75 to 85 min. The eluent was introduced by electro-spray ionization (ESI) via the nanoESI source (Thermo) using stainless steel Nano-bore emitters (40 mm, OD 1/32”, ES542, Thermo Scientific). The QExactive HF was operated in positive mode

with data dependent acquisition without the use of lock mass, default charge of 2+ and external calibration with LTQ Velos ESI positive ion calibration solution (88323, Pierce, Thermo) every 5 days to less than 2 ppm. The tune file for the survey scan was set to scan range of 350 – 1400 m/z, 120,000 resolution (m/z 200), 1 microscan, automatic gain control (AGC) of 3e6, max injection time of 100 ms, no sheath, aux or sweep gas, spray voltage ranging from 1.7 to 3.0 kV, capillary temp of 250 °C and an S-lens value of 80. For the 10 data dependent MS/MS events the loop count was set to 10 and the general settings were resolution to 15,000, AGC target 1e5, max IT time 50 ms, isolation window of 1.6 m/z, fixed first mass of 120 m/z and normalized collision energy [5] of 28 eV. For individual peaks the data dependent settings were 1.00e3 for the minimum AGC target yielding an intensity threshold of 2.0e4 that needs to be reached prior of triggering an MS/MS event. No apex trigger was used, unassigned, +1 and charges >+8 were excluded with peptide match mode preferred, isotope exclusion on and dynamic exclusion of 10 sec. In between experiments, routine wash and control runs were done by injecting 5 µl LC-MS solution containing 5 µL of 10 fmol/µL BSA or enolase digest and 1 µL of 10 fmol/µL angiotensin III (Fluka, Thermo)/oxytocin (Merck) to check the performance of the platform on each component (nano-LC, the mass spectrometer (mass calibration/quality of ion selection and fragmentation) and the search engine).

MaxQuant processing

Raw files were analyzed with MaxQuant (version v2.1.4.0).[14] The following changes were made to the standard settings of MaxQuant: Label-free quantification was enabled with an LFQ minimal ratio count of 1. Match between runs and iBAQ quantification were enabled. Searches were performed against a Uniprot database created by merging reviewed (Swiss-Prot) and unreviewed (TrEMBL) sequences (downloaded the 21st September 2022) from mus musculus (taxonomy_id:10090; 88,023 results), bacterial fucosidase (32,942 results), sialidase (73,638 results), galactosidase (146,928 results) and hexosaminidase (37,896 results). “proteingroups.txt” file was used for further modifications in Perseus (version 2.0.7.0)[15], including logarithmic transformation (log_2) and removal of proteins ‘Only identified by site’, ‘Reverse’, ‘Contaminant’ and identified based on only one peptide. Non-existing LFQ value due to not enough quantifies peptides were substituted with zero. To analyze the abundance of proteins, their label-free quantification (LFQ) intensities were

compared using GraphPad Prism (version 9.4.1 for macOS) and MetaboAnalyst (more details in "Statistical and Bioinformatics Analysis").

Caecal Short Chain Fatty acids analysis

We used a derivatization method prior to UPLC-MS analysis. Briefly, cecal contents (50 - 60 mg wet material) were homogenized in double-distilled water and then sonicated 10 min in an iced water bath. An aliquot of the resulting material (50 µL) was transferred into tubes containing acetonitrile (200 µL) and valproic acid (used as internal standard). Following incubation at -20°C (1h) the samples were centrifuged, and supernatants were transferred into glass tubes for derivatization (1 h, 40 °C) using 3-nitrophenylhyrazine in the presence of EDC and pyridine. Samples were then purified by liquid-liquid extraction using chloroform to remove the remaining reagents. The SFCA-containing samples were then analyzed using a Nexera LC 40X3 coupled to ZenoTOF 7600 instrument (from Shimadzu and Ab Sciex, respectively). The SCFA were analyzed using a Kinetex F5 (150 × 2.1 mm; 1.7 µM) column maintained at 40 °C. A gradient between H2O-ACN-acetic acid (94.9:5:0.1; v/v/v) and ACN-acetic acid (99.9:0.1; v/v) was used to separate the different isomers. For compound ionization, an ESI source operated in positive mode was used. SCIEX OS 3.0 was used for data analysis. The signal (AUC) of the different SCFA was normalized to the signal of the internal standard (valproic acid). SCFA content was normalized to the caecal content weight.

Human fecal proteomics

The MASCOT Generic Format files from previously analyzed human fecal proteomes[16] were used to identify and quantify the proteins. The MS/MS data were processed using Sequest HT search engine within Proteome Discoverer 2.5 SP1 against a human protein database obtained from Uniprot (81.579 entries January 2023) trypsin (RK) was specified as cleavage enzyme allowing up to 2 missed cleavages, 4 modifications per peptide and up to 5 charges. Mass error was set to 10 ppm for precursor ions and 0.6 Da for fragment ions. Oxidation on Met (+15.995 Da), Carbamidomethyl on Cys (+57.021 Da), pyro-Glu formation from Gln or Glu (-17.027 Da or – 18.011 Da respectively), Acetylation (+42.011Da) and Met-loss (-131.040 Da) on protein-terminus were considered as variable modifications. False discovery rate (FDR) was assessed using a target/decoy PSM validator and set to <5%. Relative quantification was

performed by taking the number of PSMs for each protein identified. Before statistical analysis, the proteomic data were filtered to only include proteins having unique peptides ≥ 2 and PSMs ≥ 3.

Statistical and Bioinformatics Analysis

Statistical analyses were performed using GraphPad Prism version 9.4.1 for macOS (GraphPad Software, San Diego, CA, USA) and RStudio version 2022.12.0+353. Data are expressed as the mean ± s.e.m. Comparison between three groups at one time-point was performed by one-way ANOVA followed by Tukey's test for normally distributed data and Kruskal-Wallis followed by Dunn's test for not normally distributed data. Comparison between three groups at different time-points was performed by 2-way repeated measures ANOVA, followed by Tukey's test. The results were considered statistically significant at $P < 0.05$. The presence of outliers was assessed using the Grubbs test.

For the gut microbiota, statistical analysis was performed using the R package mare.[17] To account for the varying sequencing depth, the number of reads per sample was used as an offset in all statistical models. Overall microbiota structure was assessed using principal coordinate analysis (PCoA) on beta diversity computed using the Bray-Curtis dissimilarity, representing the compositional dissimilarity between the samples. Significant differences between groups were tested using nonparametric multivariate analysis of variance (PERMANOVA) (*adonis* in the *vegan* package[18]). Differential abundance testing was performed using the *mare* function "*GroupTest*" with both relative and absolute abundance data fitted in generalized linear models assuming a negative binomial distribution. If the fitted model failed to fulfil model assumptions (primarily heteroscedasticity of the residuals), generalized least squares models were used. P-values were adjusted by the Benjamini-Hochberg method for multiple testing. FDR-adjusted p-values < 0.05 were considered statistically significant. As absolute microbiota measurements have been suggested to better reflect true changes,[19] log2 fold change values of absolute abundances of the significant genera identified by differential abundance testing (FDR-$p < 0.05$) were further visualized using the ggplot2 package (figure 11) .

Statistical analysis for the mouse proteomics, including non-parametric tests (Wilcoxon rank-sum test), volcano plot and principal component analysis (PCA), were done using MetaboAnalyst (version 5.0)[20]. For human proteomics, t-test was performed after data

normalization (Log transformation (base 10) and auto scaling) using MetaboAnalyst and PCA was computed from scaled data using PCA function in "FactoMineR" package. Differences between clusters were estimated by PERMANOVA test with 999 permutations on Euclidean distance using adonis2 function from "vegan" package. Proteins that were significantly up/down-regulated were used to create a gene list and execute Kyoto Encyclopedia of Genes and Genomics (KEGG) pathway and functional annotation clustering, giving which term/annotation groups were enriched (using DAVID 2021, https://david.ncifcrf.gov).[21,22] Following default settings, only clusters with P-values <0.05 (corresponding to enrichment scores ≥ 1.3) were shown in Supplemental figure 4 and 5. For human fecal proteomes, DAVID tool was also used to investigate the molecular function, biological process, KEGG pathway and diseases, as shown in figure 14.

REFERENCES

1 Nobel YR, Cox LM, Kirigin FF, Bokulich NA, Yamanishi S, Teitler I*, et al.* Metabolic and metagenomic outcomes from early-life pulsed antibiotic treatment. Nature Communications 2015;**6**:7486.

2 Lee S, Goodson M, Vang W, Kalanetra K, Barile D, Raybould H. 2'-fucosyllactose Supplementation Improves Gut-Brain Signaling and Diet-Induced Obese Phenotype and Changes the Gut Microbiota in High Fat-Fed Mice. Nutrients 2020;**12**.

3 Lee S, Goodson ML, Vang W, Rutkowsky J, Kalanetra K, Bhattacharya M*, et al.* Human milk oligosaccharide 2'-fucosyllactose supplementation improves gut barrier function and signaling in the vagal afferent pathway in mice. Food Funct 2021;**12**:8507-21.

4 Johansson ME, Gustafsson JK, Holmen-Larsson J, Jabbar KS, Xia L, Xu H*, et al.* Bacteria penetrate the normally impenetrable inner colon mucus layer in both murine colitis models and patients with ulcerative colitis. Gut 2014;**63**:281-91.

5 Rodriguez J, Hiel S, Neyrinck AM, Le Roy T, Potgens SA, Leyrolle Q*, et al.* Discovery of the gut microbial signature driving the efficacy of prebiotic intervention in obese patients. Gut 2020;**69**:1975-87.

6 Grivennikov SI, Wang K, Mucida D, Stewart CA, Schnabl B, Jauch D*, et al.* Adenoma-linked barrier defects and microbial products drive IL-23/IL-17-mediated tumour growth. Nature 2012;**491**:254-8.

7 Bolyen E, Rideout JR, Dillon MR, Bokulich NA, Abnet CC, Al-Ghalith GA*, et al.* Reproducible, interactive, scalable and extensible microbiome data science using QIIME 2. Nat Biotechnol 2019;**37**:852-7.

8 Callahan BJ, McMurdie PJ, Rosen MJ, Han AW, Johnson AJ, Holmes SP. DADA2: High-resolution sample inference from Illumina amplicon data. Nat Methods 2016;**13**:581-3.

9 Quast C, Pruesse E, Yilmaz P, Gerken J, Schweer T, Yarza P*, et al.* The SILVA ribosomal RNA gene database project: improved data processing and web-based tools. Nucleic Acids Res 2013;**41**:D590-6.
10 Jian C, Luukkonen P, Yki-Järvinen H, Salonen A, Korpela K. Quantitative PCR provides a simple and accessible method for quantitative microbiota profiling. PLoS One 2020;**15**:e0227285.
11 Jariwala PB, Pellock SJ, Goldfarb D, Cloer EW, Artola M, Simpson JB*, et al.* Discovering the Microbial Enzymes Driving Drug Toxicity with Activity-Based Protein Profiling. ACS Chem Biol 2020;**15**:217-25.
12 Jiang J. Activity-based protein profiling of glucosidases, fucosidases and glucuronidases. Doctoral Thesis 2016.
13 Kytidou K, Beekwilder J, Artola M, van Meel E, Wilbers RHP, Moolenaar GF*, et al.* Nicotiana benthamiana α-galactosidase A1.1 can functionally complement human α-galactosidase A deficiency associated with Fabry disease. The Journal of biological chemistry 2018;**293**:10042-58.
14 Tyanova S, Temu T, Cox J. The MaxQuant computational platform for mass spectrometry-based shotgun proteomics. Nat Protoc 2016;**11**:2301-19.
15 Tyanova S, Temu T, Sinitcyn P, Carlson A, Hein MY, Geiger T*, et al.* The Perseus computational platform for comprehensive analysis of (prote)omics data. Nat Methods 2016;**13**:731-40.
16 Kolmeder CA, Ritari J, Verdam FJ, Muth T, Keskitalo S, Varjosalo M*, et al.* Colonic metaproteomic signatures of active bacteria and the host in obesity. Proteomics 2015;**15**:3544-52.
17 Korpela K. mare: Microbiota Analysis in R Easily. R package version 1.0.
18 Jari Oksanen, F. Guillaume Blanchet, Michael Friendly, Roeland Kindt, Pierre Legendre, Dan McGlinn, Peter R. Minchin, R. B. O'Hara, Gavin L. Simpson, Peter Solymos, M. Henry H. Stevens, Eduard Szoecs, and Helene Wagner, vegan, https://CRAN.R-project.org/package=vegan, (accessed 14 June 2021).
19 Maghini DG, Dvorak M, Dahlen A, Roos M, Kuersten S, Bhatt AS. Quantifying bias introduced by sample collection in relative and absolute microbiome measurements. Nature Biotechnology 2023.
20 Pang Z, Zhou G, Ewald J, Chang L, Hacariz O, Basu N*, et al.* Using MetaboAnalyst 5.0 for LC–HRMS spectra processing, multi-omics integration and covariate adjustment of global metabolomics data. Nature Protocols 2022;**17**:1735-61.
21 Huang da W, Sherman BT, Lempicki RA. Systematic and integrative analysis of large gene lists using DAVID bioinformatics resources. Nat Protoc 2009;**4**:44-57.
22 Sherman BT, Hao M, Qiu J, Jiao X, Baseler MW, Lane HC*, et al.* DAVID: a web server for functional enrichment analysis and functional annotation of gene lists (2021 update). Nucleic Acids Res 2022;**50**:W216-21.

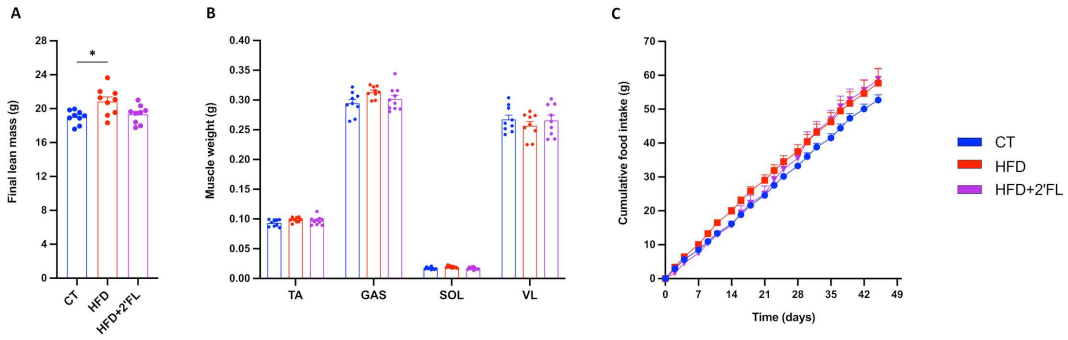

Supplemental Figure 1. (A) Final lean mass and (B) muscle weights (TA = tibialis anterior, VL = vastus lateralis, GAS = gastrocnemius, SOL = soleus). (C) Cumulative food intake. Data are means±s.e.m (n= 9-10/group). Data were analysed using one-way ANOVA for A and B and according to two-way ANOVA for C followed by Tukey post hoc test. *P < 0.05;

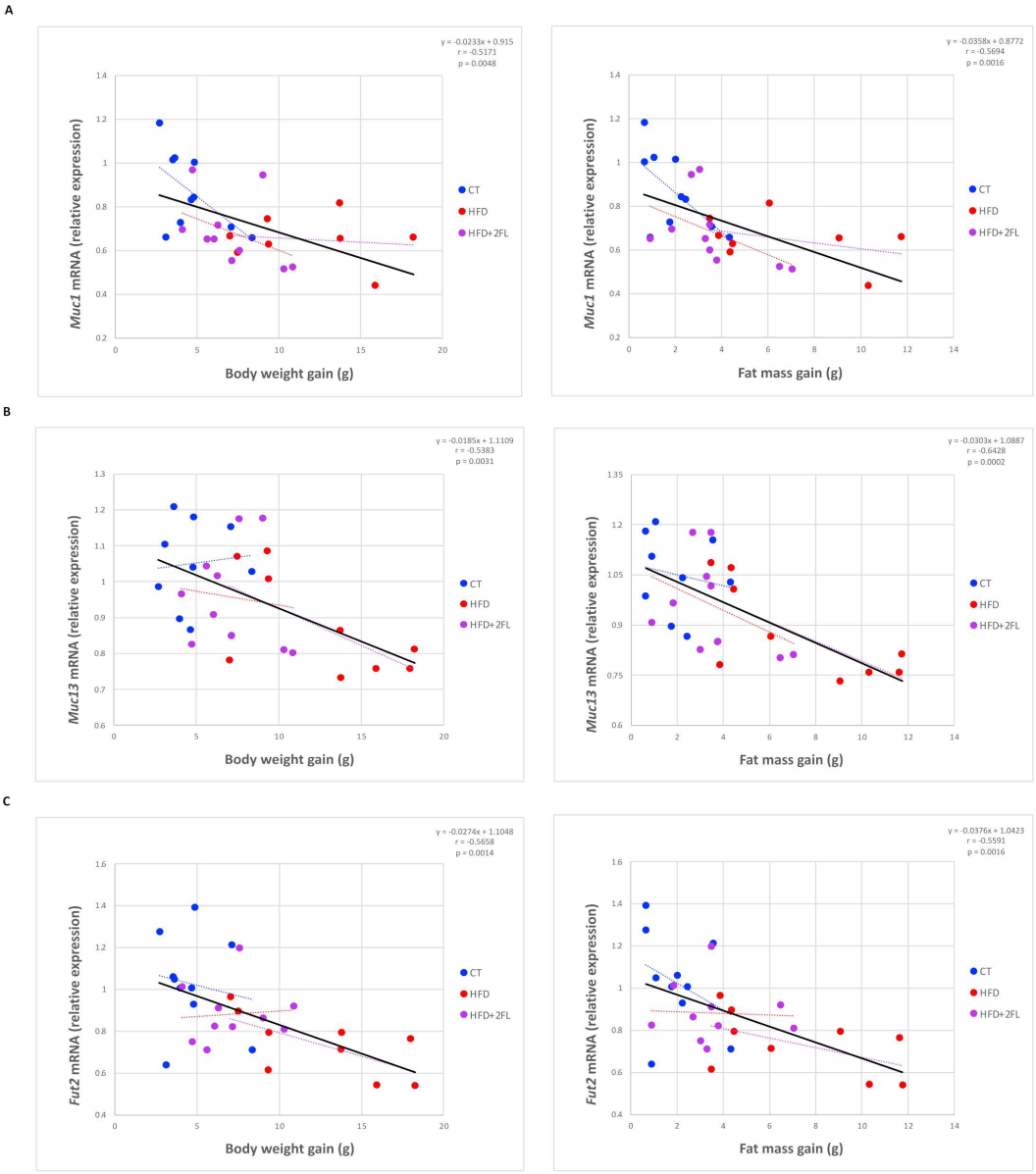

Supplemental Figure 2. Pearson correlation between mRNA colonic expression of (A) *Muc1*, (B) *Muc13* and (C) *Fut2* and body weight gain/fat mass gain (n=9-10/group).

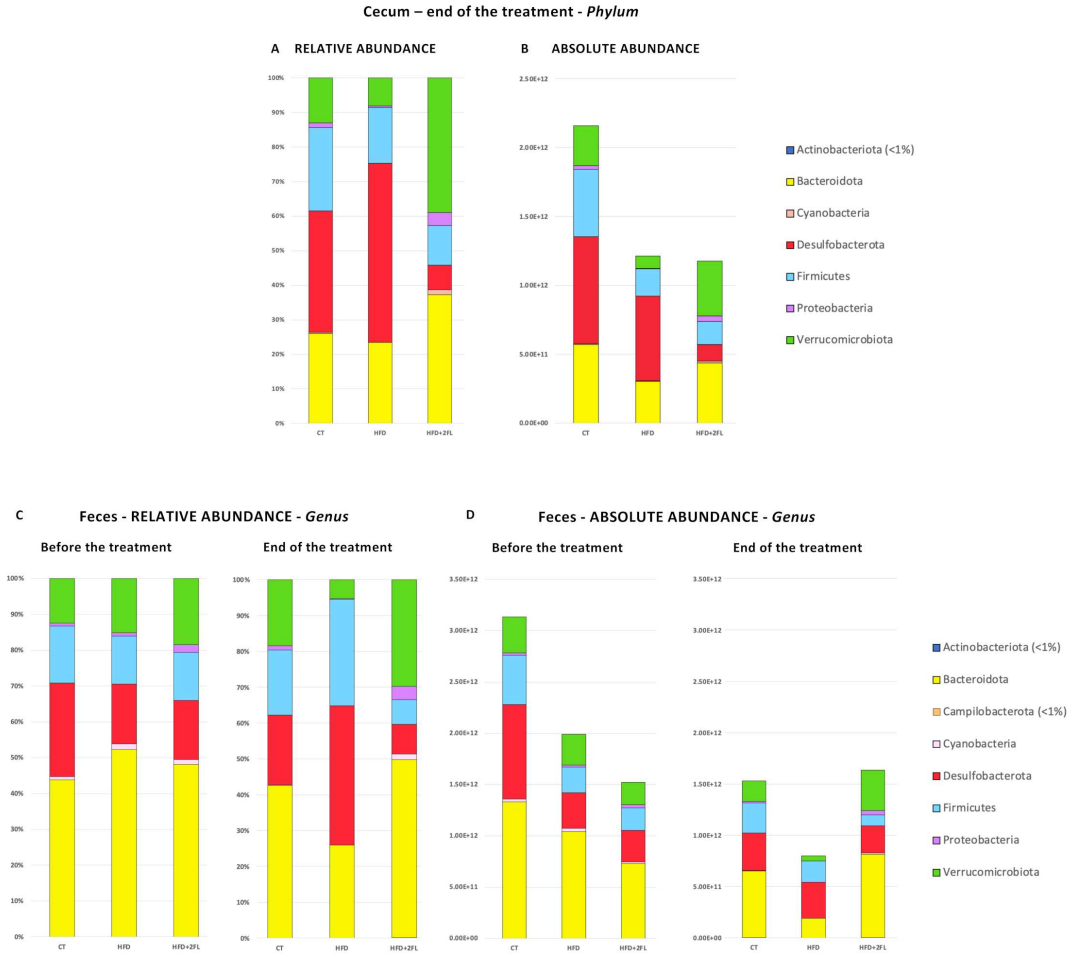

Supplemental Figure 3. (A-D) Bar graphs showing grouped taxonomic profiles of the gut bacteria at a phylum level: (A,B) relative and absolute abundance in the cecum, before and at the end of the treatment; (C,D) relative and absolute abundance in the feces, at the end of the treatment. (n= 9-10/group).

Functional Annotation Clustering

HFD vs CT

▲ UPREGULATED			▼ DOWNREGULATED		
Annotation Cluster	Enrichment Score	Term	Annotation Cluster	Enrichment Score	Term
1	9.4	**Proteolysis** **Protease** **Peptidase activity** **Hydrolase** **Hydrolase activity**	1	4.7	**Carbon metabolism** **Biosynthesis of amino acids** **2-Oxocarboxylic acid metabolism**
2	5.8	Extracellular space Disulfide bond Extracellular region	2	3.7	Extracellular region Secreted Extracellular space Signal Disulfide bond Glycoprotein
3	5.1	**Metallopeptidase activity** **Aminopeptidase activity** **Aminopeptidase**	3	3.3	**Carbon metabolism** **Metabolic pathways** **Tricarboxylic acid cycle** **Citrate cycle (TCA cycle)** **Glyoxylate and dicarboxylate metabolism** **Mitochondrion**
4	3.8	**Peptidase S1** **Peptidase S1, trypsin family, active site** **Protein digestion and absorption** **Serine-type peptidase activity** **Trypsin-like cysteine/serine peptidase domain** **Activation peptide** **Charge relay system** **Serine-type endopeptidase activity** **Tryp_SPc** **Serine protease** **Peptidase S1A, chymotrypsin-type** **Zymogen**	4	2.3	**Lipid metabolism** **Glyoxylate and dicarboxylate metabolism** **Lipid metabolic process** **Lipid catabolic process**
5	3.5	Metalloprotease Metallopeptidase activity Zinc ion binding Peptide catabolic process Metal ion binding Metal-binding Zinc	5	2.3	Pancreatic secretion Hydrolase Hydrolase activity
6	2.8	CUB 1 CUB 2 CUB domain CUB	6	1.9	**NAD binding** **Oxidoreductase activity** **Oxidoreductase** **Proton acceptor** **NAD** **Mitochondrion**
7	2.6	ZP Zymogen granule membrane Zona pellucida domain Cytoplasmic vesicle	7	1.3	Calcium Metal ion binding Metal-binding

HFD+2'FL vs HFD

▲ UPREGULATED			▼ DOWNREGULATED		
Annotation Cluster	Enrichment Score	Term	Annotation Cluster	Enrichment Score	Term
1	4.8	Extracellular space Extracellular region Secreted Signal Disulfide bond	1	4.0	**Protease** **Proteolysis** **Peptidase activity** **Aminopeptidase** **Aminopeptidase activity** **Hydrolase** **Metalloprotease** **Metallopeptidase activity** **Peptide catabolic process** **Hydrolase activity** **Zinc ion binding** **Metal ion binding** **Metal-binding** **Zinc**
2	3.4	**Carbon metabolism** **Glycolysis / Gluconeogenesis** **Biosynthesis of amino acids** **Canonical glycolysis** **Glycolysis** **Glycolytic process** **Hydroxylation**	2	2.9	CUB 1 CUB 2 CUB domain CUB
3	2.3	**Oxidoreductase activity** **Oxidoreductase** **NAD binding** **Proton acceptor** **NAD**	3	2.6	ZP Zymogen granule membrane Zona pellucida domain ZP Cytoplasmic vesicle
4	2.2	**Lipid metabolic process** **Lipid metabolism** **Lipid catabolic process**	4	2.4	Extracellular space Extracellular region Secreted
5	1.7	Myelin sheath Catalytic activity ADP binding Membrane raft Nucleotide binding Methylation ATP binding Phosphorylation Kinase activity Kinase Transferase activity Transferase ATP-binding Nucleotide-binding Nucleus	5	2.1	Cadherin 4 Cadherin 3 Cadherin 1 Cadherin 2 Cadherin Calcium Cadherin conserved site Cadherin Cadherin-like Homophilic cell adhesion CA Cell adhesion Integral component of plasma membrane
6	1.7	Cytosol Acetylation Cytoplasm	6	1.9	**Protein digestion and absorption** **Peptidase S1** **Peptidase S1, trypsin family, active site** **Peptidase S1A, chymotrypsin-type** **Trypsin-like cysteine/serine peptidase domain** **Pancreatic secretion** **Serine-type peptidase activity** **Serine protease** **Tryp_SPc** **Serine-type endopeptidase activity**
7	1.6	**Glycolysis / Gluconeogenesis** **Glycyl lysine isopeptide (Lys-Gly)** **Isopeptide bond** **Ubl conjugation**			
8	1.6	Antimicrobial Inflammatory response			
9	1.3	**Mitochondrion** **Transit peptide** **Mitochondrial matrix** **Mitochondrial inner membrane**			

Supplemental Figure 4. Functional annotation clustering performed with DAVID, showing annotation clustering, enrichment scores and terms significantly up/down-regulated by HFD and HFD+2'FL in mice. Only annotation clusters with enrichment scores ≥ 1.3 (corresponding to P-values <0.05) are shown. Terms that changed in an opposite way in HFD-fed mice compared to HFD+2'FL mice are highlighted in bold and red/blue.

Functional Annotation Clustering

Obese vs Normal subjects		
▲ UPREGULATED		
Annotation Cluster	**Enrichment Score**	**Term**
1	3.0	carboxypeptidase activity ACT_SITE:Proton donor/acceptor proteolysis Metalloprotease Carboxypeptidase Protease zinc ion binding Metal-binding Zinc
2	2.6	anchored component of membrane GPI-anchor LIPID:GPI-anchor amidated serine PROPEP:Removed in mature form Lipoprotein
3	2.6	DOMAIN:P-type 1 DOMAIN:P-type 2 alpha-1,4-glucosidase activity Starch and sucrose metabolism Glycoside hydrolase, family 31 P-type trefoil PD Galactose mutarotase-like domain Glycosidase Glycosyl hydrolase, family 13, all-beta hydrolase activity, hydrolyzing O-glycosyl compounds Galactose metabolism Glycoside hydrolase, superfamily Carbohydrate digestion and absorption Sulfation Metabolic pathways Signal-anchor carbohydrate binding apical plasma membrane Helical; Signal-anchor for type II membrane protein Lumenal Cytoplasmic integral component of membrane Repeat Helical Extracellular Transmembrane helix Transmembrane Disordered
4	2.5	proteolysis Activation peptide Protease Pancreatic secretion Protein digestion and absorption Zymogen
5	1.9	N-linked (GlcNAc...) asparagine Glycoprotein Cell membrane membrane plasma membrane Membrane

Supplemental Figure 5. Functional annotation clustering performed with DAVID, showing annotation clustering, enrichment scores and terms significantly upregulated in obese human subjects compared to normal ones. Only annotation clusters with enrichment scores ≥ 1.3 (corresponding to P-values <0.05) are shown. Terms that are similar to those enriched in HFD-fed mice are in red and some of the terms related to metabolism are highlighted in light red.

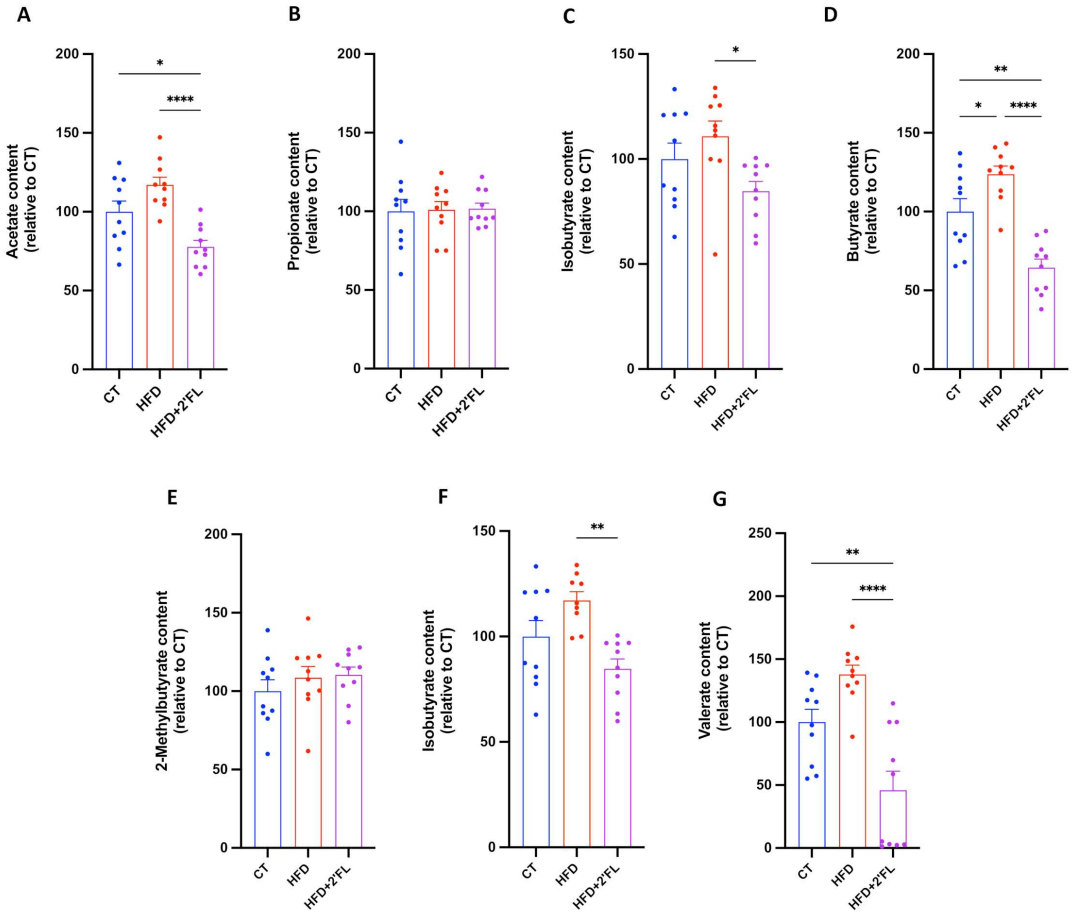

Supplemental Figure 6. Short-chain fatty acids (SCFAs) content in the cecal content. (A) acetate, (B) propionate, (C) isobutyrate, (D) butyrate, (E) 2-methylbutyrate, (F) isovalerate, (G) valerate. Data are means±s.e.m (n= 11-12/group). Data were analysed using one-way ANOVA followed by Tukey post hoc test. *P < 0.05; **P < 0.01; ***P < 0.001; ****P < 0.0001.

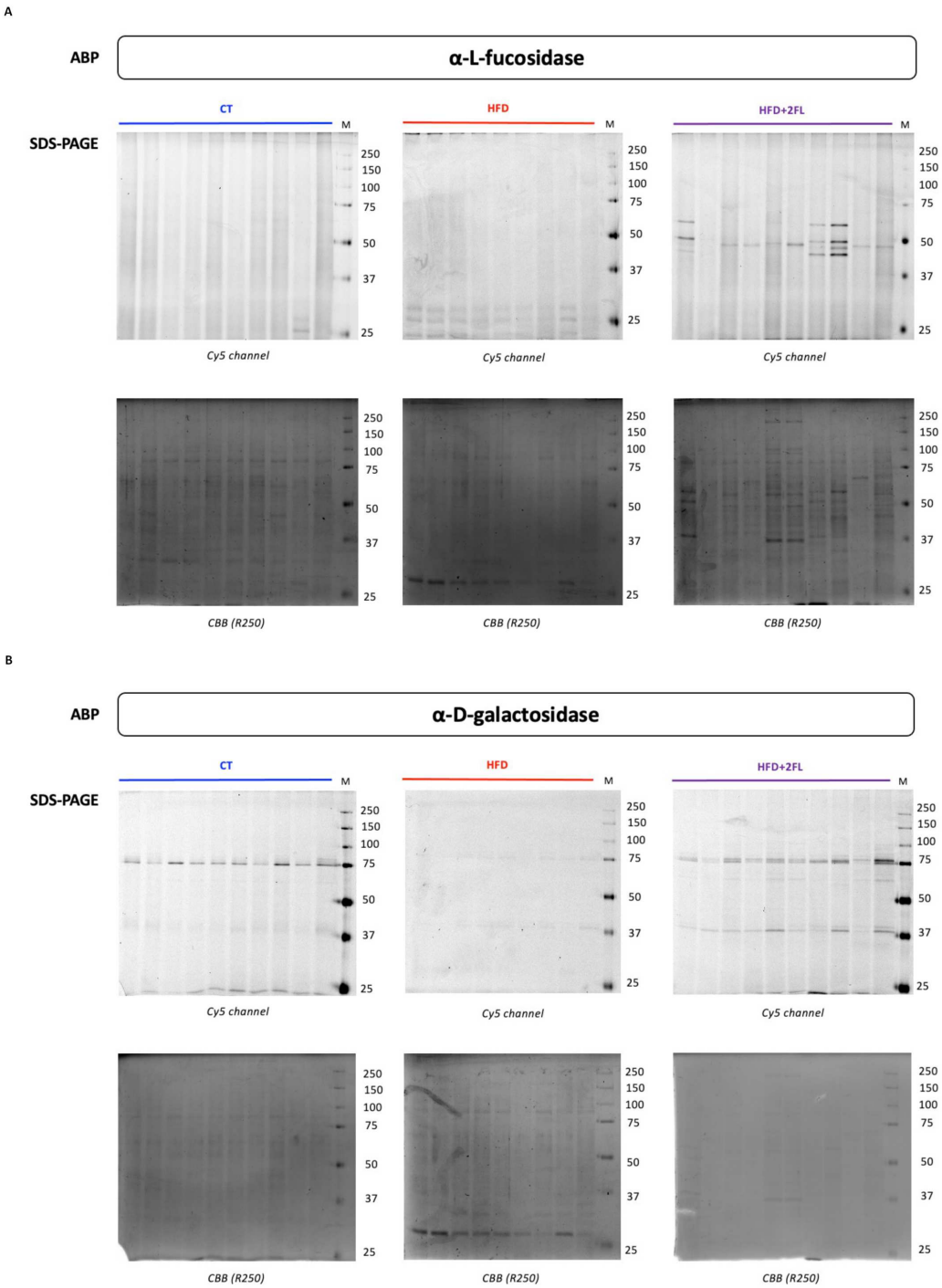

Supplemental Figure 7. In-gel fluorescent ABP labelling. (A) 1 µM for alpha-L-fucosidase labeling (JJB38 1) and (B) 0.5 µM for alpha-D-galactosidase (TB474) and their relative Coomassie Brilliant Blue (CBB) staining (n=9-10/group).

Supplemental table 9: primers sequences used for the RT-qPCR

Primers	Forward sequence	Reverse sequence
RPL19	GAAGGTCAAAGGGAATGTGTTCA	CCTGTTGCTCACTTGT
Lyz1	GCCAAGGTCTACAATCGTTGTGAGTTG	CAGTCAGCCAGCTTGACACCACG
Reg3g	CATCCACCTCTGTTGGGTTC	TTCCTGTCCTCCATGATCAAA
Pla2g2a	AAGGATCCCCCAAGGATGCCAC	CAGCCGTTTCTGACAGGAGTTCTGG
Intectin	GCACTATTGCAGAGGTCCGT	GTTGCCCCTGATTCTGCTGG
Tff3	CCCTGGTGCTTCAAACCTCT	GGGATGCTTGCTACCCTTG
Proglucagon	TGGCAGCACGCCCTTC	GCGCTTCTGTCTGGGA
Math1	CAAGTGTGTCCAGCAGTGTG	TTGAGTTTCTTCAAGGCGGC
Spdef	AGGTGCAATCGATGGTTGTG	AGGGTCTGCTGTGATGTTCA
Elf3	CCTATGAGAAGCTGAGCCGA	ACCTCTTCTTCCTTCCAGCC
Klf4	GTGCCCCGACTAACCGTTG	GTCGTTGAACTCCTCGGTCT
Hes1	CCGGCATTCCAAGCTAGAGA	GGTATTTCCCCAACACGCTC
Agr2	GCCAAAGACACCACAGTCAA	CCATCAAGGGTCTGTTGCTT
Muc1	GACATCTTTCCAACCCAGGACA	AAGAGAGACTGCTACTGCCATTAC
Muc2	ATGCCCACCTCCTCAAAGAC	GTAGTTTCCGTTGGAACAGTGAA
Muc4	CTGTGTCTGAGCTGCCTGTATT	GGGTGTCTGTGTTGATGTTGTTG
Muc13	CCCTCATCCTCATCTTGCTGATT	CTCTGCTCTTCTCCATCCTTCTTT
Muc17	CCGACACATTGCTGCTGAGAAT	GCTGTCGTCTTGGGTGCTATTT
Gcnt1	ACAGATTCAGGCTTCCTGTGATT	GCCAGGTGAGATGCCAGTTTA
Gcnt4	ATGTCCTGCAGTTCCATTGAGG	ATGTCCTGCAGTTCCATTGAGG
B3gnt6	GGCCAGATTCTCCTCTCTCAAAC	CAGTGTCGTGGGACTCTTGAAC
C1galt1	ATGGACACAGTCACCTCAAAGG	GAGGTTCTCAGCAACGTCTATGT
C1galt1c1	TCTCACGTCCAAGCCTCGT	TGTGGCCTAGCATAGTGATCAAG
Fut1	AGAATTCGCTTGCACCACCA	AAGAAGGAGCCGGCAGAGA
Fut2	TGAACTTTCGGCTAAGGTACATCT	GGAAGTGGGCCAGAGGAAAG
Fut8	AGGCGAATGGCTGAGTCTCT	TGGCCTTAACAAGCTGTTCTTCT
St3gal1	GCCCACTATGCCAGACACTT	TCAGCAGAGTCAAACCCAGC
St3gal3	TGCTGCGGTCATGTAGGAAA	CAGCGGAGTCAAGGGAAAGA
St3gal4	GGCTCTGGTCCTTGTTGTTG	TCCCTAGAACGGTTGCCAAAA
St3gal6	CACCCCAAAAGCGCAGATTTATT	CCTGCCTGAAACAGAGTCCAA
St6galnac2	CGGATGTTGTTGCTCGTTGC	AGTCGGCTCTTTCTGTTTTCC
Retnlb	CAAGGAAGCTCTCAGTCGTCAA	CACTAGTGCAGGAGATCGTCTTAG
Atg5	ATGGTTTGAATATGAAGGCACACC	TGATGTTCCAAGGAAGAGCTGAA
Atg7	CTTCCTGAGAGCATCCCTCTAATC	CGGCTCGACACAGATCATCATAG
Nlrp6	CCCGAAATGTCATCTGAGTGTTCT	TTCAGGGCCTCGGAAAGGT
Fcgbp	AACTTTGCCCACTGACCTG	CCACAGCCTCCCTGCACT
Daglb	CTCCACCAGCAACAAGACAA	GCAGTTCTCCACTTCTGCATC
Dagla	CCCTCAAGTGCTTCGCTTAC	GTCTTTGCCCAGAACCACA
Napepld	TTCTTTGCTGGGGATACTGG	GCAAGGTCAAAAGGACCAAA
Abdh4	GCACAGGGAAGAAGGTGAAG	AGCATAGACGTGGTGGGATG
Nat1	CCCCGAGTTATCGAGGATTT	CTGCAAGGAACAGAACGATG
Naaa	ATTATGACCATTGGAAGCCTGCA	CGCTCATCACTGTAGTATAAATTGTGTAG
Faah	GTGAGGATTTGTTCCGCTTG	GGAGTGGGCATGGTGTAGTT
Mgl	ATGGTCCTGATTTCACCTCTGGT	TCAACCTCCGACTTGTTCCGAGACA
Abdh6	CTGTCCATAGTGGGGCAAGT	TCAGATGGGTAGTAAGCGGC
Cb1	CTGATGTTCTGGATCGGAGTC	TCTGAGGTGTGAATGATGATGC
Cb2	CTGTGCTGCTCATATGCTGG	GCAGAGCGAATCTCTCCACT
Gpr119	AGCTCTGCTCAGCATACACAG	AAATGCCATCCGAAGGCTAC
Pparg	CTGCTCAAGTATGGTGTCCATGA	TGAGATGAGGACTCCATCTTTATTCA